Construction and Building Materials 383 (2023) 131262

Contents lists available at ScienceDirect

Construction and Building Materials

journal homepage: www.elsevier.com/locate/conbuildmat

# Investigating the Effectiveness of the Stable Measurement Tests of Self-Compacting Concrete

Fazel Azarhomayun [a], Mohammad Haji [b], Mohammad Shekarchi [c], Mahdi Kioumarsi [d,e,*]

[a] School of Civil Engineering, College of Engineering, University of Tehran, Tehran, Iran
[b] Department of Civil Engineering, Semnan University, Semnan, Iran
[c] Department of Civil Engineering, University of Tehran, Tehran, Iran
[d] Department of Engineering, Østfold University College, Halden, Norway
[e] Department of Built Environment, OsloMet - Oslo Metropolitan University, Oslo, Norway

ARTICLE INFO

*Keywords:*
Self-compacting concrete
SCC
Stability
Durability
Experimental tests

ABSTRACT

Self-compacting concrete (SCC) is a highly flowable concrete that can fill complex formwork without the need for vibration. However, its high consistency can lead to various forms of instability, such as separation, bleeding, blockage, and settling. These instabilities can adversely affect the fresh and hardened properties of the concrete. Therefore, understanding the types of instability, the factors that cause it, and the methods for measuring stability is crucial in preventing instability. However, there is currently no standardization for stability measurement methods, and their efficiency has yet to be thoroughly investigated. Furthermore, some standardized methods are expensive and time-consuming. Thus, examining proposed methods is necessary to identify valuable and efficient ones and to explore the possibility of using easier and less expensive methods instead of standardized ones.

This study aims to compare the effectiveness of different stability tests for SCC based on their reproducibility and measurability capabilities. Two types of concrete with different fluidity and stability were tested, and the relationship between the tests was investigated. The results revealed that, except for the J-ring and rocking device tests, all investigated tests yielded acceptable results for measuring SCC stability. Additionally, the effects of instability on implementing a beam-shaped mold were examined. The findings indicated that instability reduces the compressive strength, decreases the specific electrical resistance, and increases the inhomogeneity of its distribution throughout the concrete volume, thereby increasing its susceptibility to corrosion.

## 1. Introduction

Concrete instability refers to the uneven distribution of aggregates throughout the volume of concrete from the moment of mixing until the concrete reaches its hardened phase [1,2]. The high consistency of self-compacting concrete (SCC) makes it more prone to instability [3,4]. In fresh SCC, instability occurs in different forms, such as bleeding, flow blockage, segregation, and deposition of particles. The instability of fresh concrete can be influenced by various factors, such as the properties of the materials, the mix design of concrete and mortar, the density of the mixture, the shape and surface area of the reinforcement, the arrangement of the reinforcement, the height of concrete, and the pressure applied during pumping [2,5,6]. The stability of SCC is investigated through both static and dynamic categories. Static stability is defined as the ability of concrete to maintain its uniformity during casting and after the drying process. This ability itself includes resistance to bleeding, segregation, and settlement. It is to be noted that static instability causes problems on the surface and boundary layer of concrete, resulting in damage to penetration and mechanical properties. This can also reduce the cohesion between concrete and steel [6]. Dynamic stability refers to the ability of concrete to withstand the separation of its constituent parts during the mixing period, transportation, placement, and mold filling [2]. This phenomenon causes a reduction in the mechanical properties of SCC, its durability, and the continuity between rebars and concrete. The static stability of SCC is affected by various factors, including the differences in density between the aggregates and the cement paste and their geological properties. These factors depend on the inherent instability of SCC and the conditions and

* Corresponding author at: Department of Built Environment, OsloMet - Oslo Metropolitan University, Oslo, Norway.
*E-mail address:* mahdi.kioumarsi@oslomet.no (M. Kioumarsi).

https://doi.org/10.1016/j.conbuildmat.2023.131262
Received 21 October 2022; Received in revised form 27 March 2023; Accepted 30 March 2023
Available online 18 April 2023

temperature during the mixing and curing process [7].

Several experiments have been conducted to evaluate the static stability of SCC. These include the use of tests such as the statical segregation cylinder based on ASTM C1610 [8], penetration [9], segregation probe [10], electrical conductivity [11], modified penetration test [12], cylinder segregation test [12], modified segregation probe [13], numerical models [14].

With proper dynamic stability, SCC exhibits good resistance and cohesion, with large aggregates moving uniformly alongside the concrete paste [15]. However, unlike static instability, there have been relatively fewer studies on the dynamic instability of SCC, resulting in fewer standard experiments. To investigate dynamic instability, a variety of tests have been developed, including the visual instability index (VSI) [16], J-ring [17], L-box [18], V-funnel, Orimat [19], sieve aggregation [18], dynamic aggregation cylinder [20], modified L-box [21], GTM plate stability [12], density change [22,23], three-chamber sieve [24], channel flow [25], and inclined box [26], to name a few. These tests are described in detail in [27], so further explanations are avoided in this paper.

Khayat et al. [28] compared various field-oriented test methods to examine the dynamic stability of SCC. These methods included visual observation of the spread-out concrete, flow testing using different apparatus (J-ring, L-box, U-box, and V-funnel), and the pressure bleed test. The results of their study indicated that certain dynamic stability parameters affecting the passing ability of SCC could be attributed to the rheological properties of the concrete.

Felekoğlu et al. [29] conducted a study to determine the optimal parameters for achieving self-compactibility in concrete mixtures. The study involved several experiments, including slump flow, V-funnel, and L-box tests. Furthermore, the compressive strength development, modulus of elasticity, and splitting tensile strength of mixtures were investigated. It was reported that the optimal water-to-cement ratio (w/c) range for producing SCC is between 0.84 and 1.07 by volume. Choosing any ratios outside this range may result in the blocking or segregation of the mixture. This study highlights that self-compactibility test method stipulations are not universally accepted rules.

Ferrara et al. [30] employed a paste rheology model in the mix design of steel fiber-reinforced SCC. The rheological properties of cement paste and its volume ratio were optimized in the proposed methodology. The results demonstrate that this model can effectively be used to design fiber-reinforced concrete mixtures with selected fresh state properties, utilizing various ratios and types of steel fiber reinforcement.

In an experimental study conducted by Mouret et al. [31], an optimal sieve size, $D_{opt}$, is suggested, ranging from $0.5D_{max}$ to $0.625D_{max}$. Here, $D_{max}$ represents the maximum gravel size in the grading curve of concrete. This range of $D_{opt}$ ensures correct segregation analysis. This study was carried out to investigate the significance of static segregation in the column test on the fresh state of SCC. Considering total powder content (P), percentage of Fly Ash (FA), Silica Fume (SF), Limestone Powder (LP), water-to-powder ratio (w/p), and percentage of superplasticizer (SP) as input parameters, the potential of optimizing fresh properties and 28-day compressive strength of SCC was examined [32]. The output variables included powder content, slump flow, L-box (H2/H1), segregation index, and 28-day compressive strength. In total, ninety concrete mixes were designed using the central composite design (CCD) method.

Later, Patel et al. [33] conducted the Relative Slump Cone Test to fix the w/p, analyzed the hardened properties of concrete using a compressive strength testing machine, and studied the modulus of elasticity. The mixed design procedure showed satisfactory results. A review of five mixture design methods for SCC was carried out by Shi et al. [34], presenting features and flowcharts for each method. This study plays a crucial role in determining the appropriate design method for SCC.

The effects of inert and pozzolanic materials on the flowability and mechanical properties of SCC were investigated by Mahoutian and Shekarchi [35]. They recommended a new set of limits for the L-box and U-box tests for SCC containing silica fume, as the existing criteria are unsatisfactory. However, it was found that high volumes of active powders, such as metakaolin, zeolite, and silica fume, were ineffective in improving SCC's flowability and mechanical properties. Moreover, it has been found that limestone can be effectively used as filler in SCC at high volume content. The effect of using crushed dune sand and limestone filler as mineral additives in SCC has been investigated by Benmerioul et al. [36]. The results of the mechanical tests indicate that SCC containing crushed dune sand exhibits better shrinkage behavior. Nonetheless, there is a slight difference between the concrete containing limestone filler and the one containing crushed dune sand. Mehdipour et al. [37] studied the effect of inorganic additives on the fluidity and stability of self-compacting mortar under a long mixing time. The results showed that a prolonged mixing time could disperse agglomerated cement particles, leading to an increased risk of instability. Additionally, when mixing fly ash with mixtures exceeding 20%, there is a susceptibility to instability, such as separation and bleeding. However, the addition of metakaolin, which has a high membrane thickness rate, reduces the stability of the membranes and increases the mixture's cohesion. Therefore, using metakaolin in mixtures containing fly ash is beneficial to provide stability, especially when long-term mixing is involved.

The robustness of SCC is studied in a short article by Thakre et al. [38]. The fresh behavior of self-compacting recycled concrete (SCRC) with different replacement percentages of recycled concrete coarse aggregate (20, 50, and 100%) has been investigated by González-Taboada et al. [39]. Rheology is reported as the best tool to control the fresh state behavior of SCRC mixes. They reported that Bingham's 5-parameter model is suitable for describing their rheological behavior. Fresh state properties, including the rheology of rubber fiber dosed self-compacting mortar (SCM), were investigated in a study by Anil Thakare et al. [40]. Shear-thinning behavior was observed in all rubber fiber-dosed SCM mixes. It was also concluded that the inclusion of rubber fibers improved the thixotropy of SCM mixes, where the optimum flow characteristics for SCM were calculated to be 15% rubber fiber replacement. In a study by Yan et al. [41], the effect of aggregate gradation and mortar rheology on static segregation was studied by proposing a fluid-particle coupling method based on IBM to simulate SCC. It was observed that large aggregates are more likely to settle, and the settling velocity increases in larger aggregates. Stability problems are more likely to occur when the content of large aggregates is high. Yan et al. [41] proposed a fluid particle coupling technique to study the effect of aggregates and mortar on the static isolation of SCC by comparing the results of different aggregates and rheological properties of mortar. They found that the settling velocity increased with increasing the aggregate size, and SCC was more prone to stability issues when the proportion of large aggregates was high. Furthermore, the stability of mortars played a significant role in SCC segregation, with higher yield stress resulting in improved SCC stability. Although plastic viscosity had little effect on mortars, increasing the plastic viscosity of the mortar decreased the velocity of aggregate sedimentation. Suprakash et al. [42] provided a comprehensive review of the impact of calcium and silica-rich supplementary blends on SCC properties.

In the case of steel slag SCC, the workability and stability properties were investigated in detail in a paper by Pan et al. [43]. It was reported that SCC with a content of 20% steel slag sand exhibited similar workability performance to that of SCC with natural aggregates.

The rheological properties of SCC, combined with a powder-viscosity modifying admixture, were investigated based on a series of experimental studies by Li et al. [44]. The study revealed that the shear thickening of SCC could be reduced by initially mixing the aggregate and water before adding other raw materials. It was also demonstrated that the yield stress increases when there is direct contact between aggregate and water, owing to the large amount of free water absorbed by the aggregate system. Furthermore, the study presented additional

constraints necessary to achieve appropriate fluidity and low shear thickening behavior in SCC. A modified K-slump test method was developed by Bouziani [45] to evaluate the workability and static stability of SCC. To achieve proper workability and static stability, they proposed gravel to sand ratio of 1 and a gravel 3/8 to gravel 8/15 ratio of 0.6. Moreover, to comprehend the formulation and stability of a mixture created in the laboratory or in situ, Aghziel Sadfa et al. [46] developed a novel experimental procedure that characterizes both the spreading and segregation of SCC. The risk of segregation as a function of the rheological parameters of the SCCs was determined. As the key finding, it was revealed that several properties of the SCC, such as slump flow diameter, V-funnel flow time, L-box blocking ratio, sieve stability, and the mechanical response (including the compressive strength at 1, 7, and 28 days) can be regarded as influential parameters. The significant challenges and opportunities related to SCC, including sustainability, robustness, compatibility of constituent materials, modeling of flow, and virtual mix design, are assessed by Geiker and Jacobsen [47].

Liu et al. [48] presented a study on support time in double-shield tunnel boring machines (TBM) based on SCC backfilling material. A comprehensive analysis of the surrounding rock deformation and supporting system stress concluded that an optimal supporting time for backfilling self-compacting concrete backfilling material plays a critical role in reducing the deformation of surrounding rock and the risk of TBM jamming. Additionally, it enhances the stability of the surrounding rock.

Several experimental investigations have been conducted to measure the stability of SCC, with a specific focus on a single aspect of SCC instability. As a result, the findings of these studies may not be generalizable. Although any of the introduced tests can be utilized based on the literature review, it is generally necessary to perform multiple measurement methods regarding concrete stability and consider the most notable form of instability for further experimental and numerical investigations. Therefore, this research aims to explore the effectiveness of standardized and proposed tests, examine the correlation between the results of various tests, and compare the impact of instability on concrete properties with the workshop mode simulation method. Moreover, the proposed test is employed to analyze the risk of segregation as a function of the rheological parameters of SCCs.

## 2. Experimental scheme

### 2.1. Materials

The cement used in this section is Portland Cement Type II, following the ASTM C150 [49], with a specific gravity of 3.15 N/m$^3$. The chemical composition of cement is summarized in Table 1. The study utilized river sand as a fine-grained material, possessing a fineness modulus of 3.6 and a water absorption rate of 3.2%. The granulation of this sand can be observed in Fig. 1. The distribution of coarse and fine aggregates adhered to the guidelines specified by ASTM C136 [50] and ASTM C33 [51]. In addition, the study employed a third-generation superplasticizer consisting of Polycarboxylate and possessing a specific gravity of 1.1 N/m$^3$.

### 2.2. Mix design

This research considers two levels of stability and consistency for the specimens. In order to achieve the desired consistency and desired level of stability in the experimental program, 15 mixing designs were created by utilizing two groups of aggregates, varying w/c, and utilizing different grades of cement to ensure uniformity in the results. Two optimal designs were selected from these 15 mixing designs that met the specified objectives. The specifications for these two designs can be found in Table 2. The high water content scheme is denoted as HS-S, while the low water content scheme is denoted as LS-S.

### 2.3. Test methods

To ensure accuracy and consistency, each experiment was conducted a minimum of three times for each design, following the guidelines specified in ASTM C192 [52]. Furthermore, both slump flow and column tests were carried out on each design to ensure that the conditions remained within the desired range. Additionally, penetration tests, as well as tests utilizing modified probes and modified L-boxes, were performed on the experimental designs.

After selecting the appropriate mixing design for each experiment, three specimens, each consisting of 90-liter concrete, were produced. All tests were conducted simultaneously on the three designs. From each design, six cubic molds with dimensions of 10×10×10 cm were obtained, and the compressive strength of three of these molds was measured after seven days, while the remaining three were tested after 28 days. The tests conducted on the 90-liter concrete mixes and the number of repetitions are outlined in Table 3.

The process for manufacturing concrete was as follows: (a) the aggregates, cement, and stone powder were cast into the mixer, (b) water and plasticizer were gradually added, (c) the mixer was turned off for four minutes, (d) water was added, and the mixer was turned on, (e) the mixer was turned off and allowed to rest for three minutes, and (f) the concrete was mixed for an additional three minutes.

### 2.4. Reproducibility calculation

Per ASTM F1469-11 [61], the degree of similarity between the results obtained from an independent experiment using the same method, specific materials, and conditions is referred to as reproducibility. The formulas employed to calculate reproducibility coefficients are outlined in Table 4. These coefficients and relative error calculations are used to compare the reproducibility of the tests. The reproducibility results for each test can be found in Tables 5 and 6.

## 3. Comparison of the results

To compare the reproducibility of tests conducted on concrete mixes with varying levels of fluidity and stability and to assess the correlation between the test results, two levels of stability and fluidity were selected for the specimens (namely HS-S and LS-S). A summary of the results obtained from the tests conducted on the LS-S and HS-S concrete mixes can be found in Tables 5 and 6. As demonstrated in both tables, the slump flow test yielded more precise results than the J-ring test for measuring the opening diameter in both mixtures. Furthermore, in terms of measuring the level of indentation on the concrete surface, the modified probe exhibited more precise results than other comparable methods in the LS-S mixture, while the probe test was more accurate in the HS-S mixture.

In addition, in Fig. 2, the obtained values of the variables $E_{90\%}$is compared to the relative error for the HS-S design. The figure illustrates

**Table 1**
Chemical composition and physical properties of cement.

| Composition | $SiO_2$ | $Al_2O_3$ | $Fe_2O_3$ | CaO | MgO | $SO_3$ | $Na_2O$ | $K_2O$ | $C_3S$ | $C_2S$ | $C_3A$ | $C_4AF$ |
|---|---|---|---|---|---|---|---|---|---|---|---|---|
| (%) | 21.80 | 4.00 | 3.92 | 65.30 | 1.500 | 1.41 | 0.17 | 0.54 | 64.00 | 14.00 | 4.00 | 12.00 |
| Weight loss due to heat | | | | Specific density | | | | Blaine (m$^2$/kg) | | | | |
| 0.49 | | | | 3.15 | | | | 295.00 | | | | |

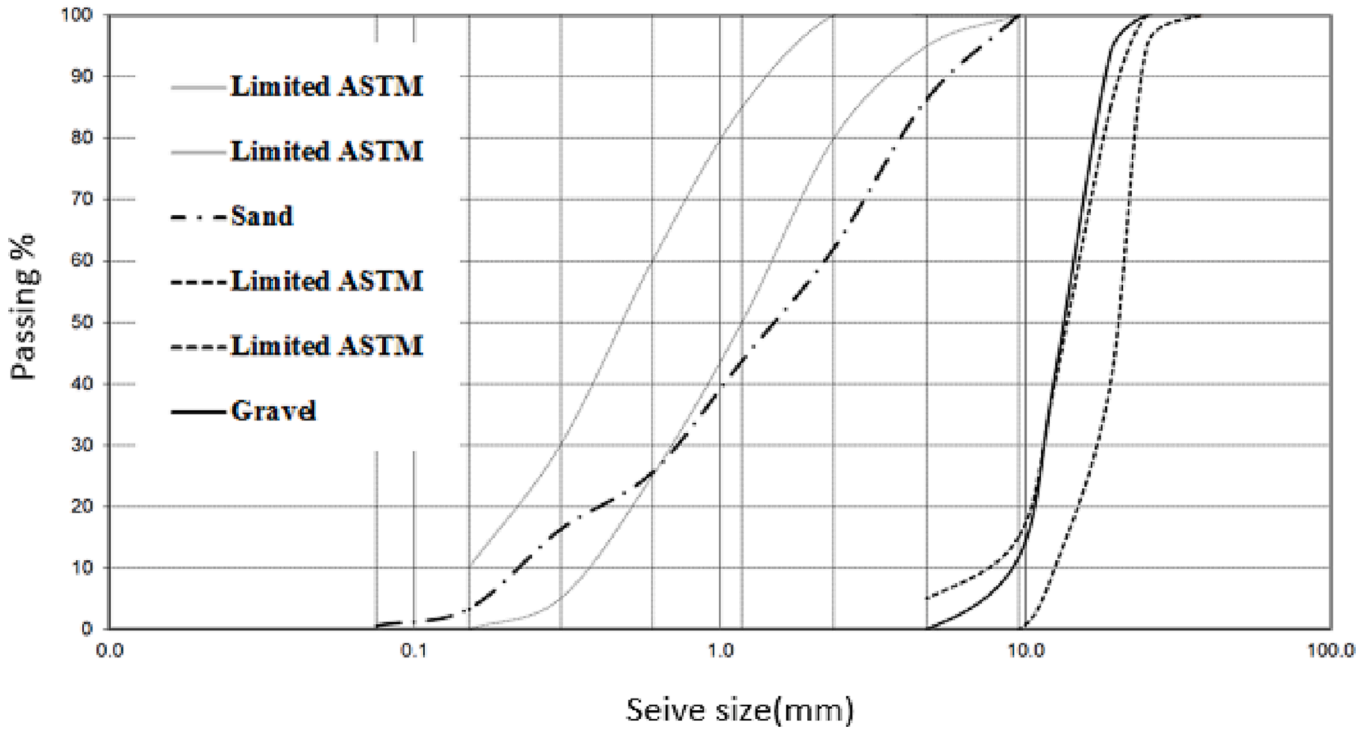


**Fig. 1.** Grading curve for concrete aggregate.

**Table 2**
Mix design of the self-consolidating concrete.

| Scheme name | Target column index | Target slump (cm) | Water (kg/m$^3$) | Cement (kg/m$^3$) | Stone powder (kg/m$^3$) | w/c | Fine aggregate (kg/m$^3$) | Coarse aggregate (kg/m$^3$) | Super plasticizer (kg/m$^3$) |
|---|---|---|---|---|---|---|---|---|---|
| LS-S | <10.00 | 60.00 ± 2.50 | 172.00 | 400.00 | 100.00 | 0.43 | 1334.00 | 445.00 | 4.00 |
| HS-S | 10.00–30.00 | 70.00 ± 2.50 | 200.00 | 500.00 | 100.00 | 0.40 | 1236.00 | 412.00 | 3.75 |

**Table 3**
Number of test repetitions for 90-liter concrete mixes.

| Test | Slump flow ASTM C1611 [53] | Column ASTM C1610 [54] | J-ring ASTM C1621 [55] | Modified L-box [56] | Probe [57] | Modified probe [58] | Penetration ASTM C1712-09 [59] | Tilt box [60] |
|---|---|---|---|---|---|---|---|---|
| No. of repetitions | 4 | 2 | 1 | 1 | 2 | 2 | 2 | 1 |

**Table 4**
The employed formulas for reproducibility.

| | |
|---|---|
| Calculate the coefficient of variation (COV) | $COV = \frac{Mean}{Standard\ deviation}(\%)$ |
| Calculation of $E_{90\%}$(error with 90% confidence margin) | $E_{90\%} = C \times \frac{\sigma}{\sqrt{n}}$ |
| Calculate the relative error | $Relative\ Error = \frac{E_{90\%}}{x}$ |
| Using dimensionless coefficients | $Dimensionless\ Response = \frac{R - R_{min}}{R_{max} - R_{min}}$ |

three parameters: J-spr, which represents the opening radius value of the J-ring, J-diff, which indicates the height difference between the inside and outside of the J-ring; and JR-diff, which represents the difference between the opening radius of concrete and its unconstrained state.

### 3.1. Measurement capability

The capacity of a testing device to precisely measure changes in a specimen due to external parameters is referred to as measurement capability. A dimensionless parameter known as the standardized response mean (SRM) is employed to evaluate this ability for two groups of responses from a single experiment. Higher SRM values indicate that the difference in the average of the parameter under investigation is more significant than the difference in the standard deviation, enabling the device to detect changes in the target parameter. Thus, an increase in the value of SRM indicates a higher capacity of the device to measure effectively.

The error values are elicited from each experiment better to understand the difference between the two experimental schemes. Fig. 4 compares the slump effect on the errors of the experiments in the LS-S and HS-S designs. Figs. 3 and 4 demonstrate that all the tests, except for the height difference between the inside and outside of the J-ring and the tilt box, exhibit high SRM values. These high SRM values indicate that the tests could effectively differentiate between the two mixtures. A comparison of the SRM values obtained from the tilt box and the

**Table 5**
The results of the tests performed on the LS-S mixture.

| Test | Measured parameter | Average | Standard deviation | Error ($E_{90\%}$) | Standard deviation | Relative error | Minimum acceptable range | Maximum acceptable range |
|---|---|---|---|---|---|---|---|---|
| Slump flow* | Opening diameter | 62.60 | 0.12 | 1.47 | 2.00 | 2.34 | 20.00 | 85.00 |
| J-ring (J-spr) | Opening diameter | 59.80 | 1.49 | 1.75 | 2.50 | 2.93 | 20.00 | 85.00 |
| J-ring (J-diff) | The difference in height outside and inside the ring | 3.50 | 2.42 | 2.87 | 68.30 | 80.35 | 0.00 | 8.50 |
| J-ring (JR-diff) | The difference between the diameter of the slump and the J-ring | 2.75 | 2.33 | 2.73 | 86.40 | 99.57 | 0.00 | 50.00 |
| Probe* | The amount of indentation in the concrete surface | 0.23 | 0.12 | 0.08 | 51.90 | 42.69 | 0.00 | 10.00 |
| Modified probe* | The amount of indentation in the concrete surface | 0.20 | 0.09 | 0.06 | 44.70 | 36.79 | 0.00 | 10.00 |
| Penetration* | The amount of indentation in the concrete surface | 0.21 | 0.12 | 0.07 | 54.00 | 44.38 | 0.000 | 5.00 |
| Separation column | SI | 8.41 | 3.08 | 2.06 | 36.60 | 24.57 | 0.00 | 200.00 |
| Tilt box* | The difference in penetration head depression in concrete before and after the flow cycle | 0.90 | 0.14 | 0.17 | 15.70 | 18.49 | 0.00 | 6.80 |
| Locking index of L-box | The ratio of concrete height at the beginning and end of the machine | 0.82 | 0.07 | 0.08 | 8.50 | 10.10 | 0.00 | 1.00 |
| Modified L-box index | L-box test index | 0.05 | 0.06 | 0.07 | 13.10 | 154.80 | 0.00 | – |

* The unit of numbers is a centimeter.

**Table 6**
The results of the tests conducted on the HS-S mixture.

| Test | Measured parameter | Average | Standard deviation | Error ($E_{90\%}$) | Coefficient of variation | Relative error | Minimum acceptable range | Maximum acceptable range |
|---|---|---|---|---|---|---|---|---|
| Slump flow* | Opening diameter | 70.30 | 3.06 | 1.50 | 4.40 | 2.10 | 20.00 | 85.00 |
| J-ring (J-spr) | Opening diameter | 64.75 | 4.17 | 4.90 | 6.40 | 7.500 | 20.00 | 85.00 |
| J-ring (J-diff) | The difference in height outside and inside the ring | 2.50 | 2.41 | 2.83 | 96.40 | 113.40 | 0.00 | 8.50 |
| J-ring (JR-diff) | The difference between the diameter of the slump and the J-ring | 6.50 | 1.68 | 1.98 | 26.00 | 30.50 | 0.00 | 50.00 |
| Probe* | The amount of indentation in the concrete surface | 1.04 | 0.55 | 0.30 | 52.90 | 28.90 | 0.00 | 15.00 |
| Modified probe* | The amount of indentation in the concrete surface | 1.17 | 0.73 | 0.40 | 62.40 | 34.11 | 0.00 | 12.50 |
| Penetration* | The amount of indentation in the concrete surface | 0.80 | 0.50 | 0.24 | 59.90 | 29.40 | 0.00 | 5.00 |
| Separation column | Segregation index | 14.45 | 5.10 | 2.79 | 35.40 | 19.30 | 0.00 | 200.00 |
| Tilt box* | The difference in penetration head depression in concrete before and after the flow cycle | 0.92 | 0.19 | 0.23 | 50.50 | 24.10 | 0.00 | 6.80 |
| Locking index of L-box | The ratio of concrete height at the beginning and end of the machine | 0.60 | 0.18 | 0.13 | 30.20 | 23.30 | 0.00 | 1.00 |
| Modified L-box index | L-box test index | 0.94 | 0.43 | 0.35 | 45.90 | 37.60 | 0.00 | – |

*The unit of numbers is a centimeter.

modified L-box index indicates that the modified L-box is more sensitive to changes in fluidity. Conversely, the tilt box is not sensitive to mixtures with relative static stability but differing fluidity. This lack of sensitivity can be attributed to the tilt box's simulation of concrete pumping, shaking, and impact, which measures concrete stability in response to these actions. On the other hand, the modified L-box test simulates the state of concrete after being pumped, flowing, and filling sections.

## 4. Comparison of the test errors

This chapter compares the errors in various tests and discusses the relationships between penetration tests, probe tests, and modified probe tests. In addition, the separation column test, modified L-box test, and tilt box test are compared to shed light on their differences.

### *4.1. The effect of concrete fluidity on the repeatability of the tests*

According to Fig. 5, the error values of the tests generally increase with an increase in consistency, but the amount of increase differs in each test. The tests of slump flow, column, and the difference of the opening radius of concrete with the unrestricted state show the slightest change compared to the consistency change. However, the tests of the L-box (blocking ratio) and the value of the opening radius of the J-ring have the most significant error increase after the consistency increase.

### *4.2. Relationships between penetration tests: probe, modified probe, and penetration tests*

This section compares the results of the probe, modified probe, and penetration tests, which have similar performances. The purpose of all three tests is to estimate the level of concrete stability by measuring their indentation on the top surface.

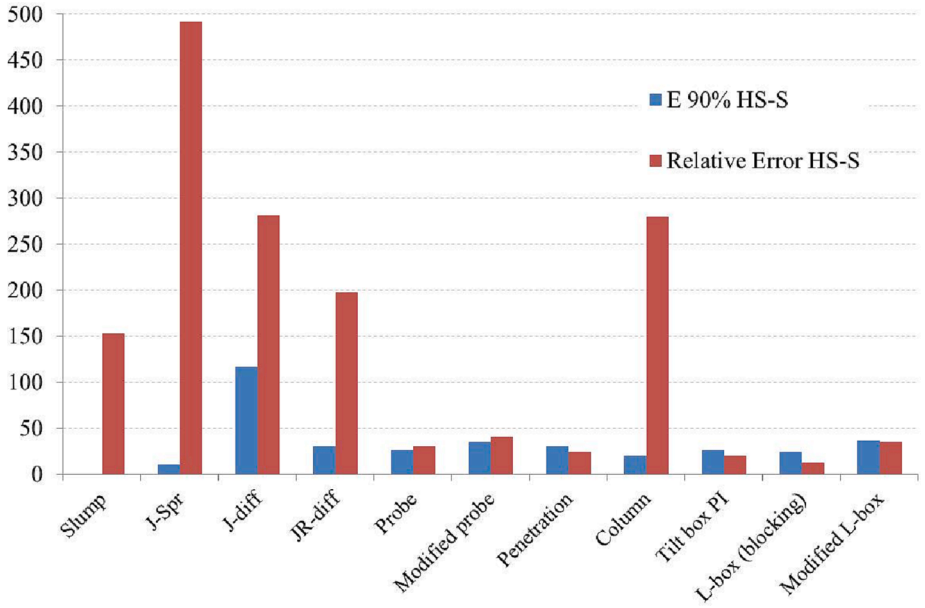


**Fig. 2.** Comparison of $E_{90\%}$ and relative error of the performed tests for HS-S design.

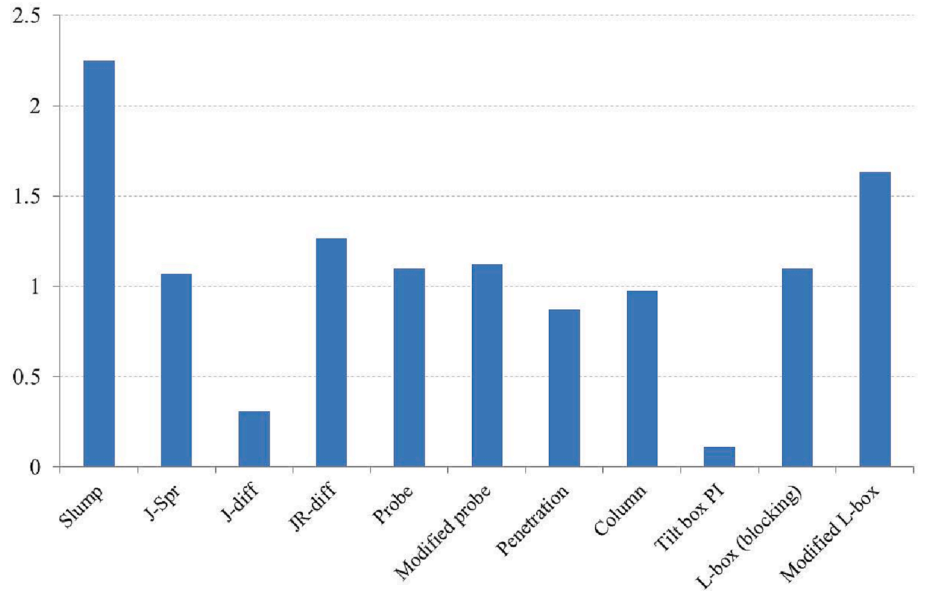


**Fig. 3.** SRM of the experimental tests performed in this research.

Fig. 6 demonstrates a linear relationship between the probe and modified probe test results, with a correlation coefficient of 0.93. Furthermore, both tests yield higher values as the slump flow increases. The reason is the reduction of concrete yield stress in mixtures with higher slump values. Decreasing the yield stress reduces the threshold for solid particle sedimentation and increases the instability of concrete. The slight increase in instability between the two designs has led to a corresponding increase in probe penetration into the HS-S design. Therefore, it is recommended to use the modified probe test instead of the probe test since it does not exhibit asymmetry or skewing issues when testing relatively unstable specimens. As shown in Fig. 7, the penetration test has a linear relationship with a suitable correlation coefficient with these two tests. Because of this high correlation and considering the fact that the probe and modified probe tests have an error of less than 5% (which means their high reproducibility) and due to the simplicity of construction, their results can be used instead of penetration devices.

Since all three tests are highly correlated, they can be used interchangeably. However, the modified probe test is recommended due to the simplicity of its device construction and symmetric testing conditions.

### 4.3. Review of separation column test

This section discusses the relationship between the separation index obtained from the separation column test and other tests.

Fig. 8 illustrates a linear and direct relationship between the probe test and the separation column index with a correlation coefficient of 0.76. Fig. 9 shows a linear relationship between the separation column index and the modified probe test, with a correlation coefficient of 0.4. Based on the criteria of the American Concrete Society Committee 237 report [1], which considers a column separation index of less than 10%

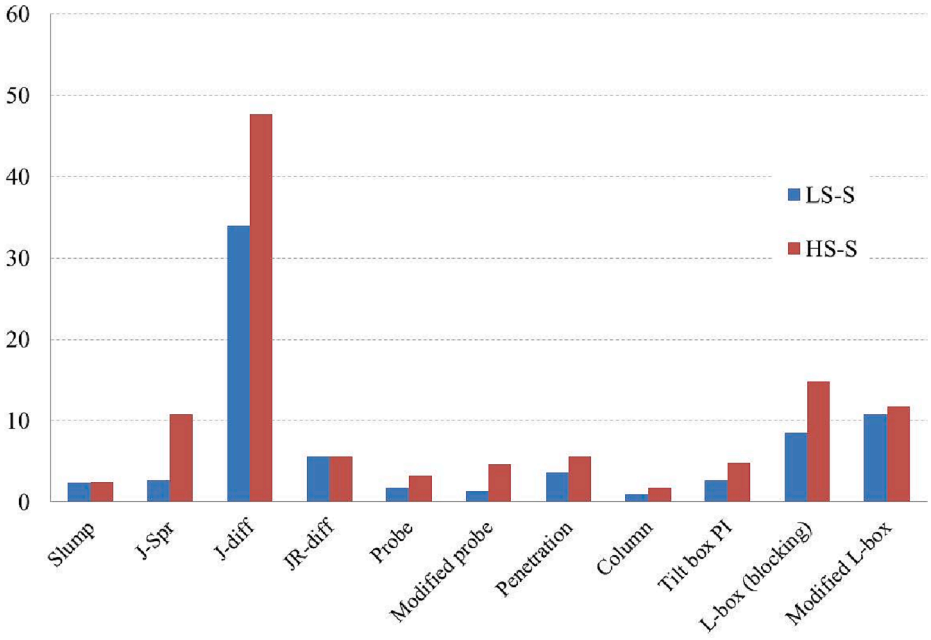


**Fig. 4.** Comparison of slump effect on the errors of experiments in two designs, for LS-S and HS-S.

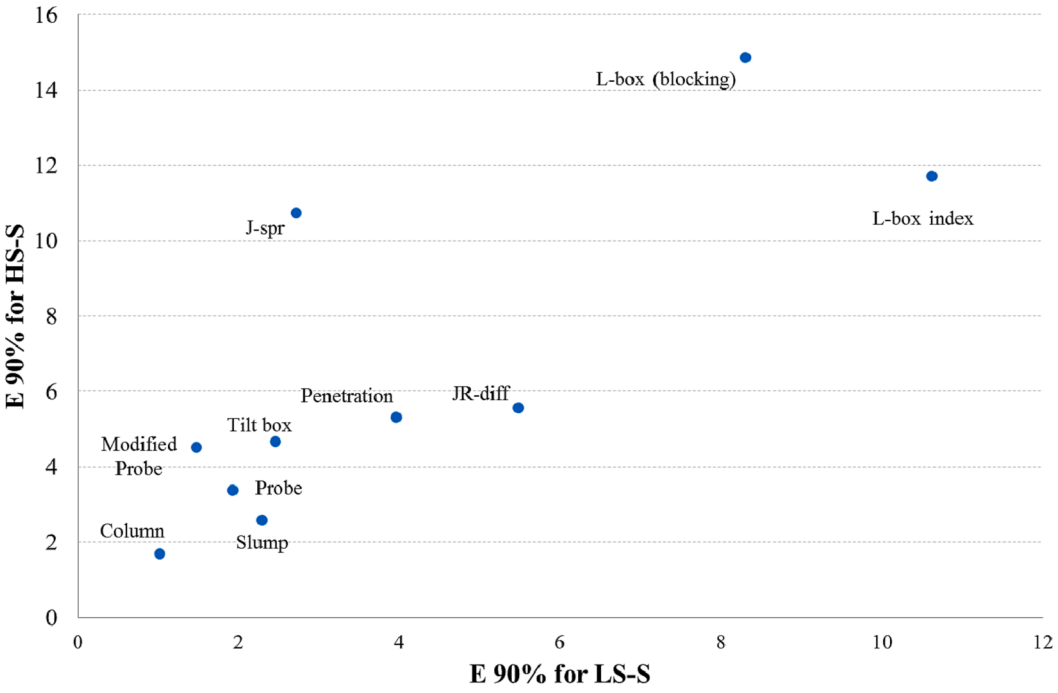


**Fig. 5.** Comparison of errors of the tests on two designs, LS-S and HS-S.

as stable, it can be concluded that both the probe and modified probe tests used in this study achieve the critical value of 6 mm.

Fig. 10 compares the separation column index with the blocking index of the L-box. The relationship between the blocking index and the modified blocking index of the L-box is also shown in Fig. 10. An increase in the probability of blockage and a decrease in flow rate result in a reduction in the blocking index. Conversely, a decrease in the blocking index indicates an increase in the probability of non-uniformity and the occurrence of dynamic instability in the modified L-box. As shown in the figure, the blocking index does not necessarily decrease and may even increase with an increase in instability. As mentioned before, concrete may fall into the vertical section when it flows, causing it to be very close to the horizontal area of the measured surface at the bottom of the horizontal section. This phenomenon is illustrated in Fig. 11(a) and (b).

In general, if the number reported for the blocking index is lower than 0.5, it indicates that the concrete is unstable. However, even if this index is too large, it does not necessarily mean that the concrete is stable. More data, including the experimental observations, is needed. Therefore, using the L-shaped box experiment alone is not recommended to evaluate the instability of SCC.

Fig. 12 shows a linear relationship between the values obtained for the static separation index and the modified L-box index. Increasing the static separation enhances the probability of dynamic interaction caused by the concrete motion in the absence of external energy. This

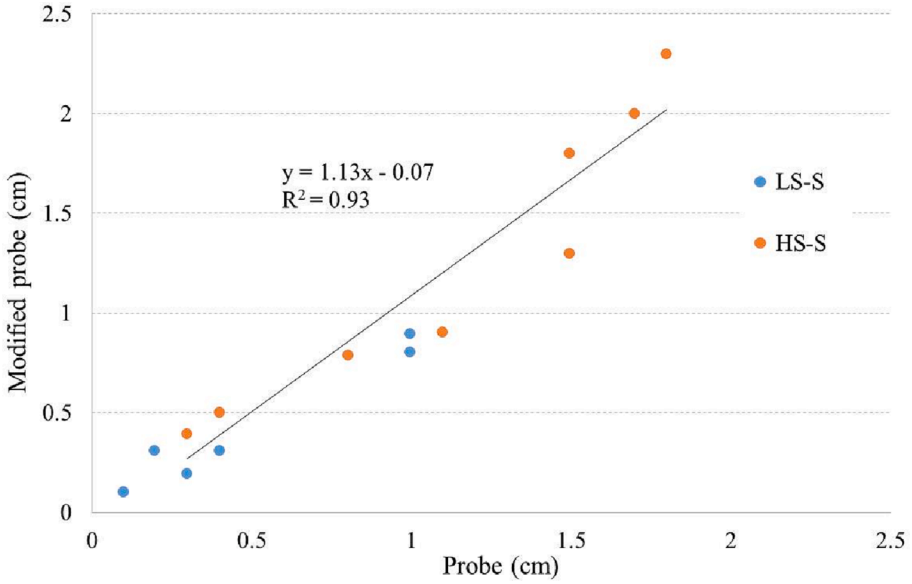


**Fig. 6.** Relationship between the probe and modified probe tests.

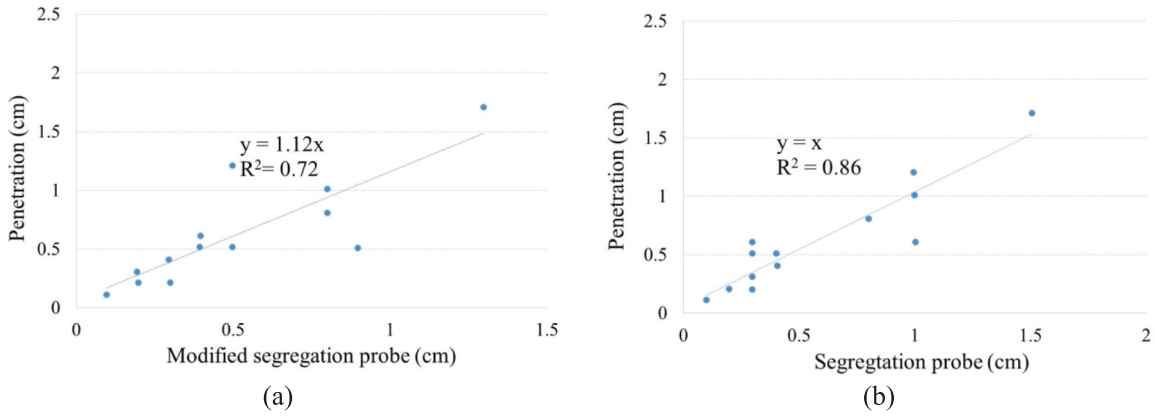


**Fig. 7.** Relationship of the penetration test with (a) probe test and (b) modified probe test.

relationship, in contrast to the index obtained for tilt box, which was related to the separation column index of cement and the flow of concrete, is not related to the stress state or cement grade and depends only on the stability of the specimen. The dynamic stability of concrete against motion caused by its weight is strongly influenced by the static stability of concrete, which is also related to preventing the aggregates from collapsing under their weight. Therefore, concrete that can resist inertia and collapse within the matrix can prevent the loss of aggregates in the flow due to weight.

### 4.4. Modified L-box test review

It is shown that when the blocking index is around 0.6, the value of the modified blocking index of the L-box may be one or more, leading to an increase in the occurrence of dynamic instability. Figs. 13 and 14 illustrate the relationship between the modified L-box index and surface infiltration tests. As depicted in the figures, the previous tests have a linear relationship with a correlation coefficient greater than 0.5. This also confirms the conclusion of the last section that the dynamic stability measured by this index depends on static stability estimated by surface infiltration tests and can be substituted by modified probe experiments. The critical value of the proposed dynamic instability for the modified L-box index corresponds to a 1-cm penetration of the modified probe.

As depicted in Fig. 15, upon comparing the outcomes of the modified L-box and the rocking system, both of which examine dynamic stability, no discernible correlation was observed between the results of these two experiments. This discrepancy could be due to the disparate conditions of each experiment and the measured variables. It appears that the rocking system, which operates by measuring the state of stroke, evaluates concrete's stability against external energy sources in general. On the other hand, the modified L-box index measures the uniform distribution of concrete while flowing through the reinforcement and without the input of external energy. Hence, the concrete's response to these two phenomena could potentially differ.

### 4.5. Tilt box test review

The tilt box is designed to measure the ability of the concrete to maintain dynamic stability after the impact of external energy on the concrete.

Fig. 16 shows the effect of the initial penetration of the compliance device on the separation probe. Due to the similarity in the test procedure, the initial penetration of the tilt box can be considered a surface infiltration experiment. The linear relationship of the separation probe test, with a correlation coefficient of 0.73, has also been verified. Based on the correlation between two variables, it is possible to utilize the

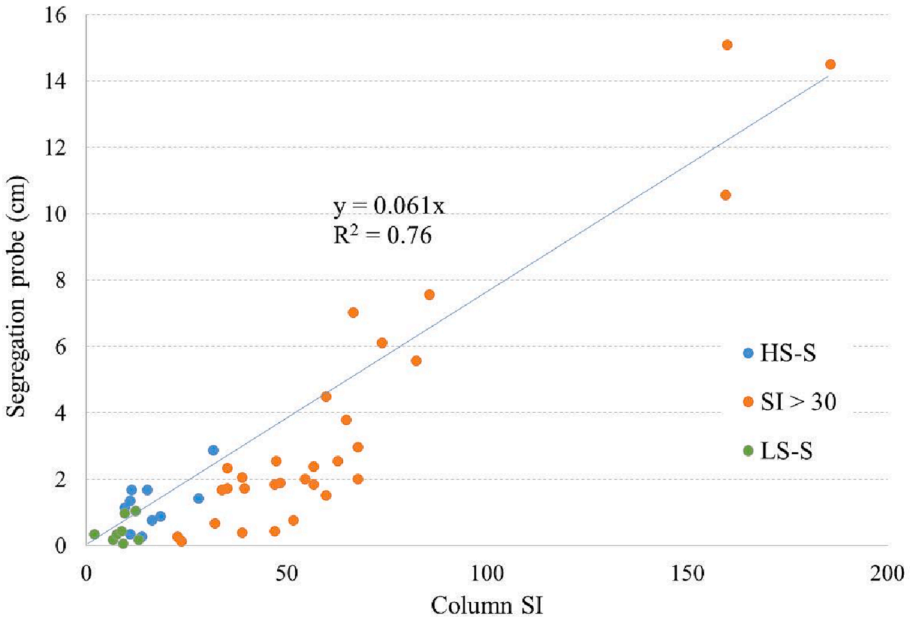


**Fig. 8.** Relationship between the probe test and separation column index.

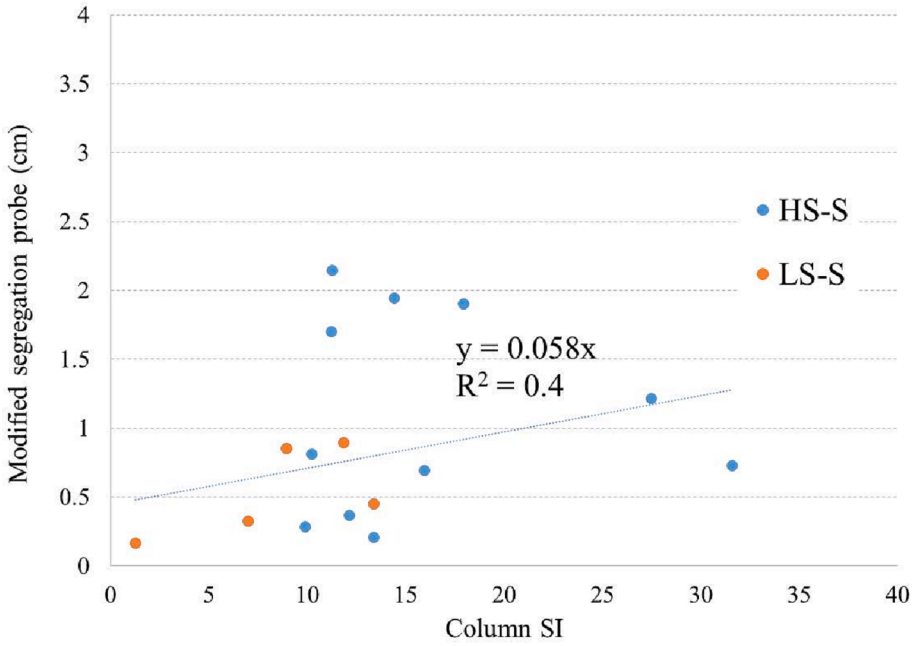


**Fig. 9.** Relationship of modified probe test with separation column index.

critical value of 1.2 cm for the initial penetration of the indentation in the case of the rocking experiment instead of the 6 mm critical value obtained for the modified probe in the previous section. Because of this relationship, the characteristics of the surface penetration test can be considered valid in the case of the variable of initial indentation penetration. For instance, as demonstrated in Fig. 17, when the flow rate is raised, the initial penetration of the specimen's indentation device (PI) also increases. However, the penetration depth index (PDI) decreases. This can be attributed to the higher cement grade in the specimen with greater slump flow and the mixture's ability to maintain homogeneity after external energy is applied.

Fig. 18 compares the tilt box PDI with the separation column index (SI) and the modified Separation probe (cm). As demonstrated in this figure, there is no proper correlation between this index and static separation tests. Consequently, this index does not necessarily relate to the concrete's overall static stability.

However, when comparing the penetration index of the LS-S and HS-S designs with the separation column index separately, each design exhibits a linear relationship with the separation column index. For instance, Fig. 19 compares the tilt box penetration index of the tilt box test for the LS-S design with the column separation index. In this study, the two indexes demonstrate a linear relationship with a correlation coefficient of 0.92. This suggests that, for a given concrete flow and grade of concrete, the measured dynamic stability obtained from the penetration index of the tilt box experiment is dependent on the static stability of concrete.

The penetration index of the rocking experiment measures the dynamic stability at impact and after the application of external energy,

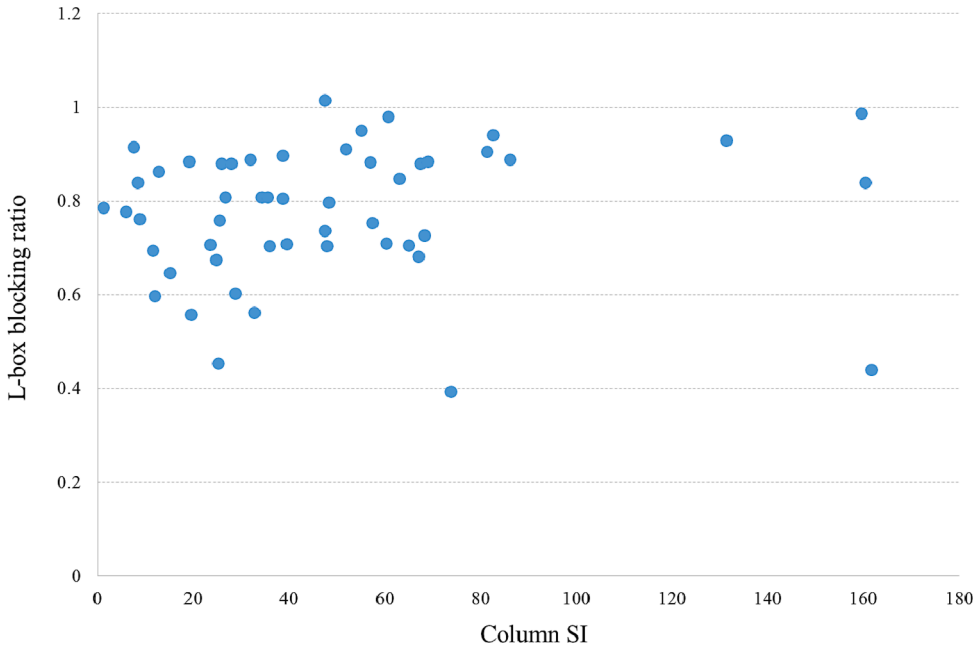


**Fig. 10.** Comparison of the separation column index and L-box blocking index.

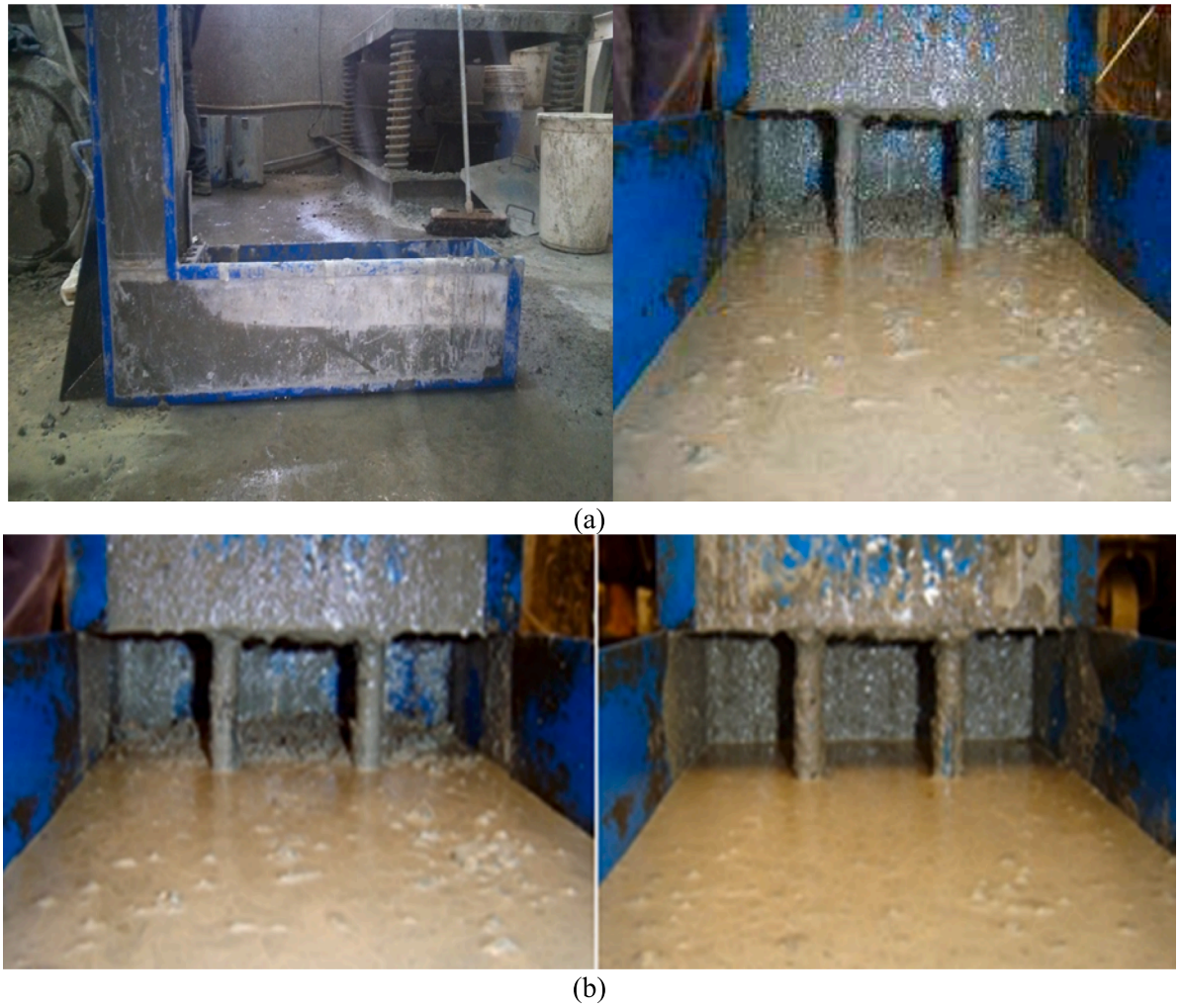


**Fig. 11.** The separation in concrete, while leachate has passed, produces a leveled surface.

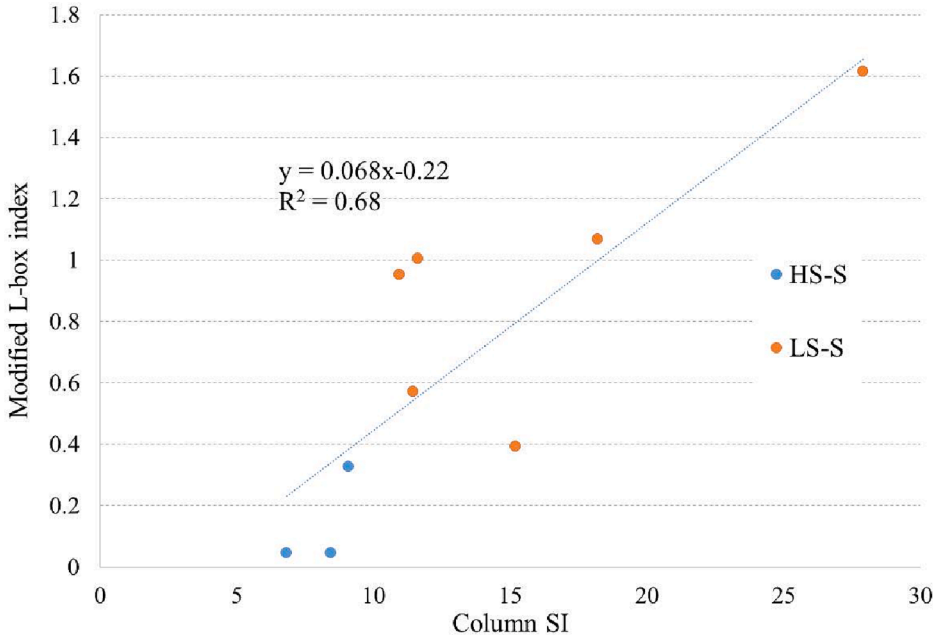


**Fig. 12.** Relationship between separation column index and modified L-box index.

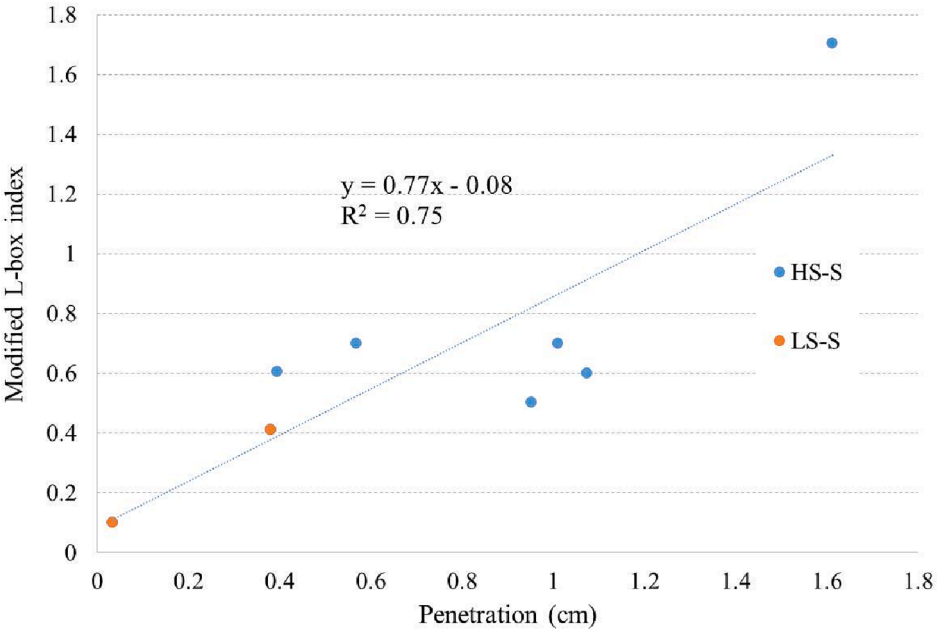


**Fig. 13.** Relationship between modified L-box index and the penetration test.

and the cement content and concrete flow influence its dependence on static stability. The above explanations regarding nearly stable concrete (with a column index of less than 15) have been reviewed, and Esmaeilkhanian et al. [26] have also studied durable concrete with a visual stability index (VSI) of equal to or less than 1. Nevertheless, further investigation is required for highly unstable concrete.

### 4.6. Column separation and modified L-box tests review

The separation column and modified L-box tests require fresh concrete to be washed on sieve no. 4 (i.e., 4.75 mm). However, this process is time-consuming, requires at least two people, and involves high water usage. Therefore, during the seven designs of the HS-S code, the aggregates that passed sieve no. 4 were passed through two sieves with larger pore sizes (6.3 and 9.5 mm), and the remaining aggregates were weighed. This process was carried out to assess the aggregate distribution when stagnant in the separation column index and when in motion in the L-box. In the following sections, each of these two experiments will be considered.

#### 4.6.1. Column separation test

In the separation column test, concrete is cast into a column divided into three parts. As time passes, the concrete on the top and bottom parts is separated, washed on the sieve, and the separation index is calculated using their weight. Fig. 20 shows the weighted averages of the aggregates of different sizes in the lower and upper sections of the separation column. As expected, the weighted values of the same-size aggregates are higher in the lower section.

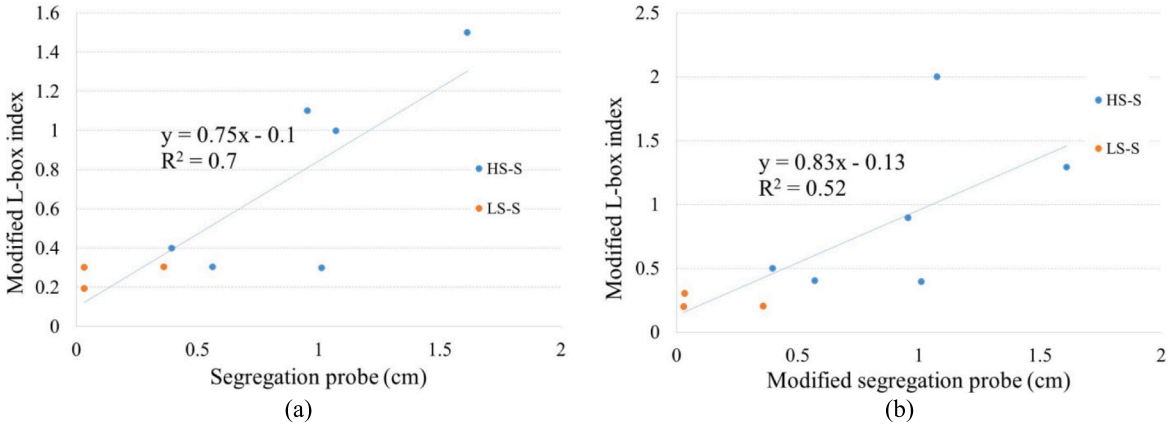


**Fig. 14.** Relationship between modified L-box and (a) segregation probe test, and (b) modified probe tests.

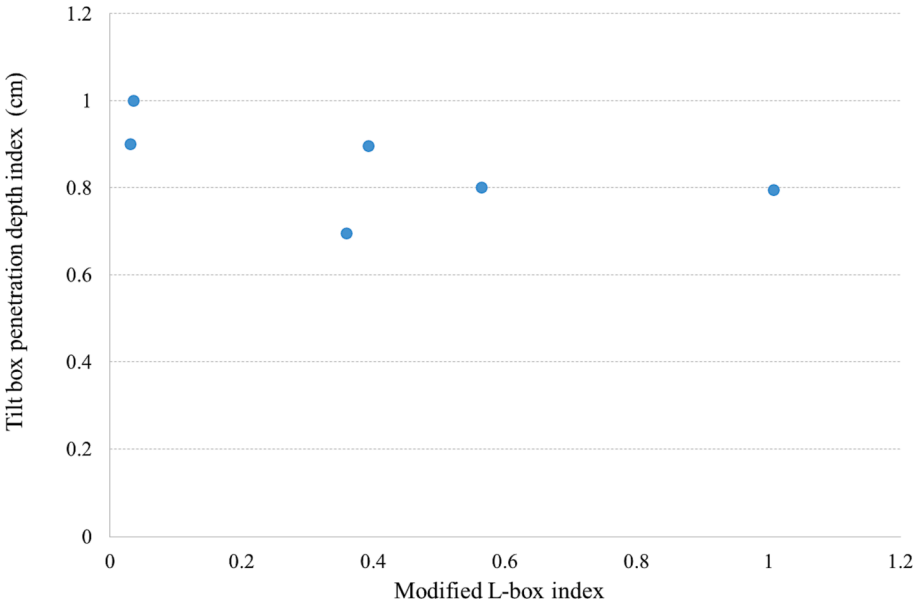


**Fig. 15.** Relationship between the modified L-box and tilt box penetration index, the unit is in cm.

Fig. 21 depicts the average percentage of aggregate distribution with different sizes in the upper and lower sections of the separation column. The larger particles in concrete (larger than 9.5 mm in size) have a higher weight percentage in the lower section of the column, while the aggregates with sizes between 4.75 and 6.3 mm have a higher weight percentage in the upper section of the column. This indicates that the larger particles are expected to settle in the lower parts of the concrete volume.

*4.6.2. Modified L-box test*

In the modified L-box test, the concrete is divided into four sections, and each section is washed separately on a sieve. The weight of the aggregate that remains on each sieve is used to calculate the modified L-box index. The different parts of the box are labeled in Fig. 22.

According to the results of the separation column test, six experiments were conducted on the remaining aggregates on sieve no. 4 (i.e., 4.75 mm) using the HS-S code designs. After weighing the aggregates, they were passed through sieves with pore sizes of 6.3 and 9.5 mm to determine the distribution of aggregates within the concrete volume. Fig. 23 shows the average weighted values of the aggregates for each section.

Fig. 24 displays the average weight percentage of aggregates of different sizes in each section. Based on this figure, it can be observed that in the absence of blockage (which was not observed in the projects examined in this section), the smallest percentage of aggregates larger than 9.5 mm is found in the L4 area, which is closest to the vertical portion of the device. This may be due to the larger mass and inertia of the larger particles, resulting in more time for them to come to a halt in the motion of the concrete matrix after the opening of the box apparatus.

Fig. 25 compares the Turgut separation index [21] with the modified index calculated using the method described in Section 5.6.2. The figure reveals that the modified index produces higher values than the Turgut index method. However, it can also be observed that the modified index reaches a critical instability point within the same limit values suggested by Turgut, where the concrete is likely to be unstable when the index value falls between one and two.

To calculate the modified L-box index using the Turgut method, it is necessary to determine the initial ratio of coarse aggregates. If the L-box index is calculated using the Turgut method and the values of residual aggregates on the sieve with a size of 9.5 mm (sieve number 8.3) are used, the calculation of the new index must include the initial volume ratio of aggregates with particle sizes greater than 9.5 mm that were used in the mixing scheme. Fig. 26 compares the index values calculated by the Turgut method for aggregates with particle sizes greater than 9.5

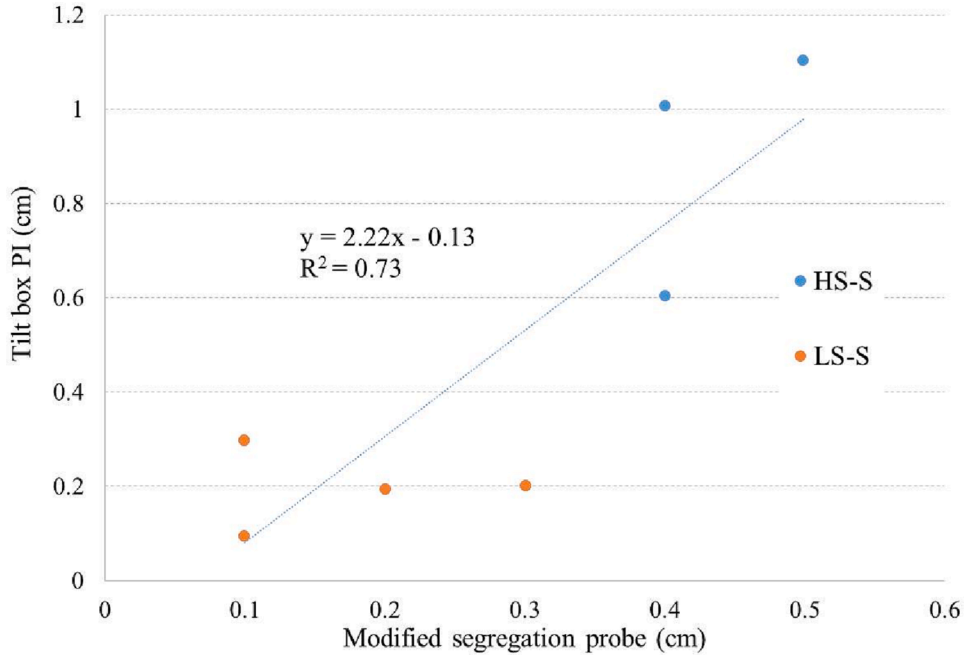


**Fig. 16.** Relationship between the modified separation probe and tilt box penetration index.

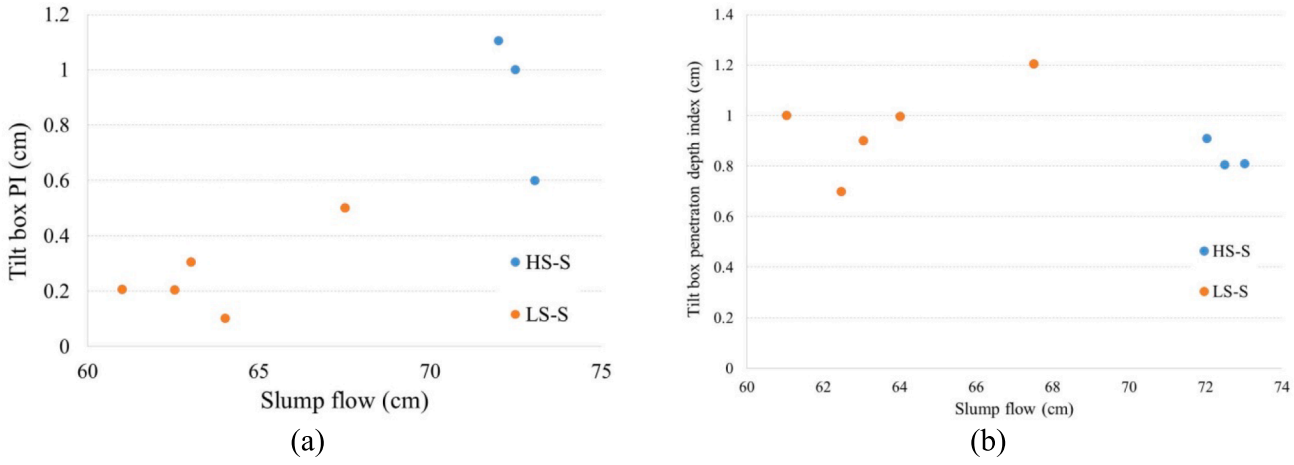


**Fig. 17.** Comparison of the slump flow with (a) tilt box penetration index, and (b) tilt box penetration depth index.

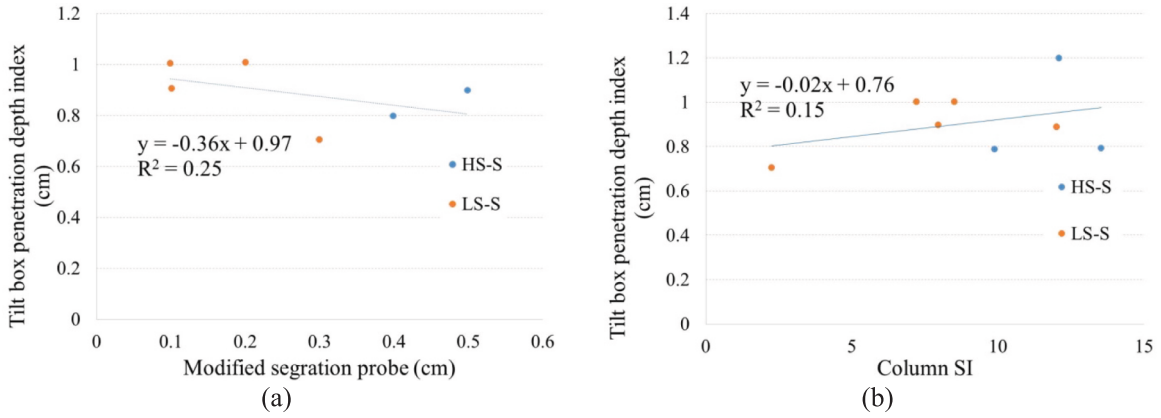


**Fig. 18.** Comparison of the tilt box penetration depth index with (a) the modified separation probe, and (b) the separation column index (SI).

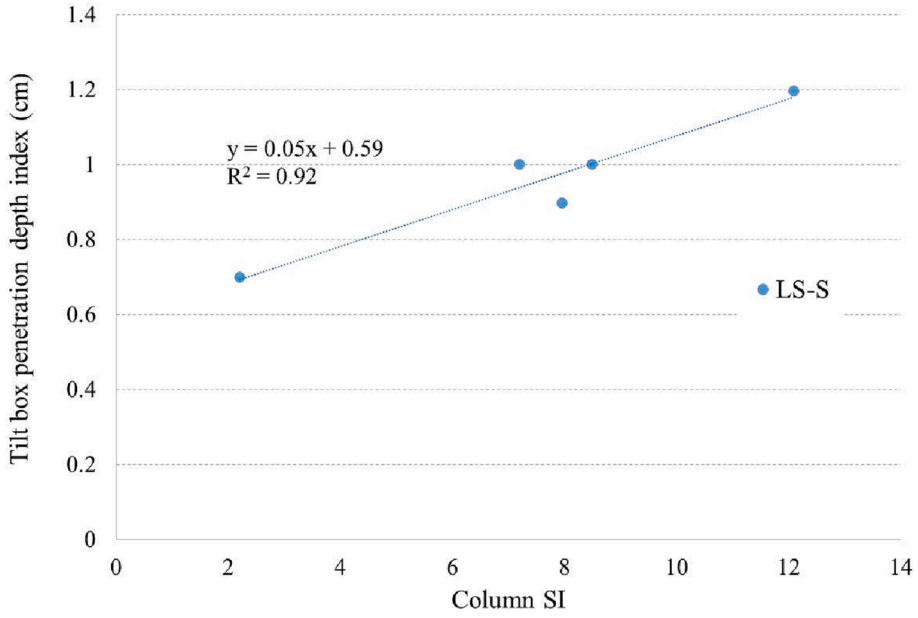


**Fig. 19.** Comparison of the tilt box penetration depth index and column SI, the unit is in cm.

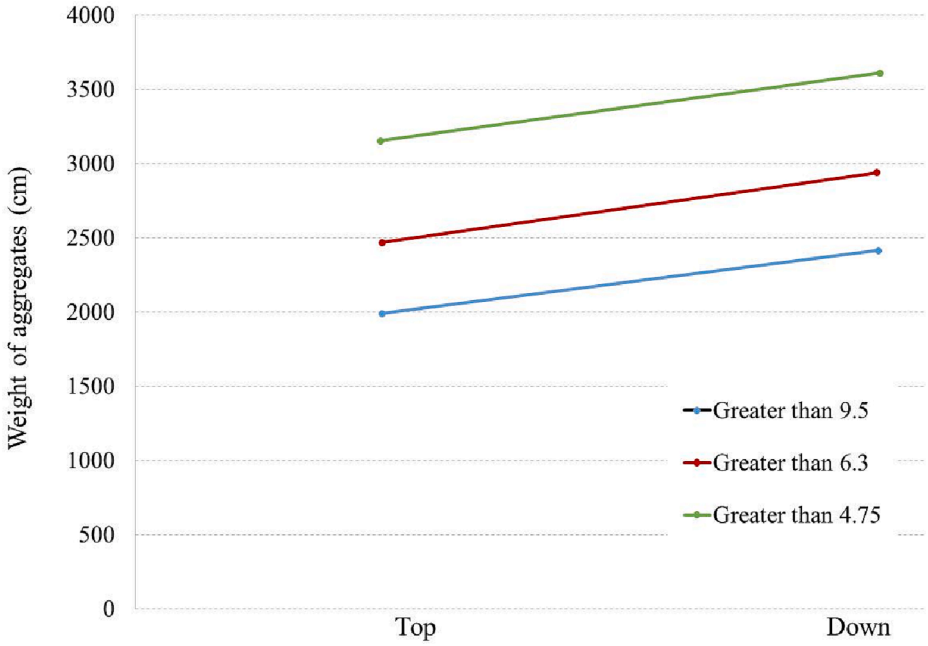


**Fig. 20.** The average weighted of the aggregates with different sizes in the lower and higher sections of the separation column.

mm and coarse aggregates with particle sizes greater than 4.75 mm. As shown in Fig. 25, these two indices are unrelated, and sieve number 3.8 cannot be used in place of sieve number 4 to compute the modified L-box index when using the Turgut method.

When calculating the modified L-box index, it is not necessary to use the initial ratio of coarse volume to the whole concrete. Instead, the modified index can be computed using aggregates of size greater than 9.5 mm in place of aggregates greater than 4.75 mm, which will give the modified index for aggregates on sieve 3.8. Fig. 27 compares the modified index values for aggregates greater than 9.5 mm with the indices for the volume of the coarse aggregates greater than 4.75 mm.

As illustrated in Fig. 27, the two indices show a linear correlation with each other, with a correlation factor of 0.9. This indicates the feasibility of using the remaining aggregates on sieve 4 to calculate the modified L-box index. However, in this case, the critical limit must be altered to 0.6 for susceptible unstable concrete and 0.95 for unstable ones. Fig. 28 presents the average percentile of the aggregate distribution of various sizes in the concrete of the upper and lower sections of the column separation test, considering all seven experiments mentioned.

## 5. Effect of stability levels on beam specimens

Experimental tests were carried out on intermediate-scale beams to study the effect of the mentioned parameters. Two concrete beams with a constant cement grade and w/c were constructed with different stability levels. Twelve samples were collected from each beam to examine and compare variables such as apparent density, specific electrical

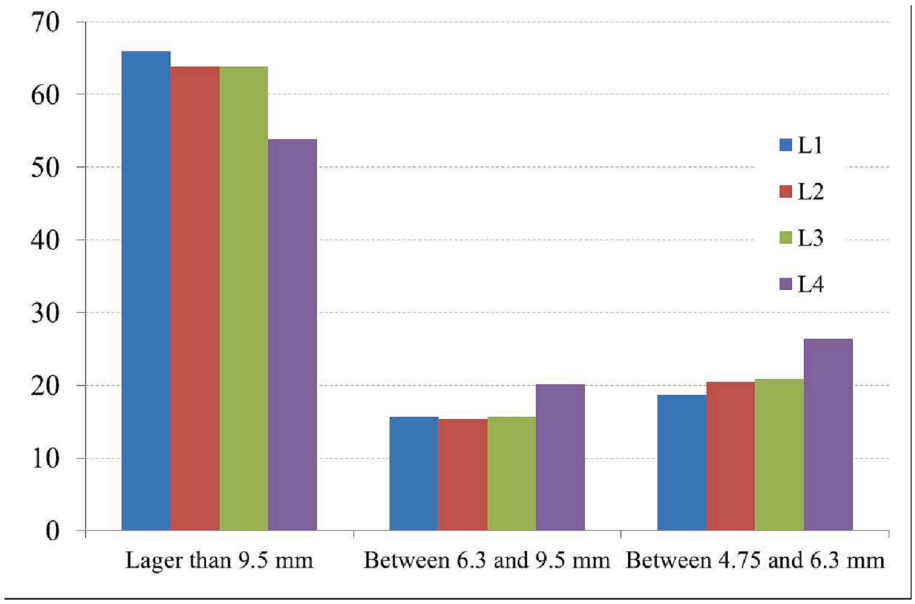


**Fig. 21.** The average distribution percentage of aggregates of different sizes in the concrete parts of the L-box.

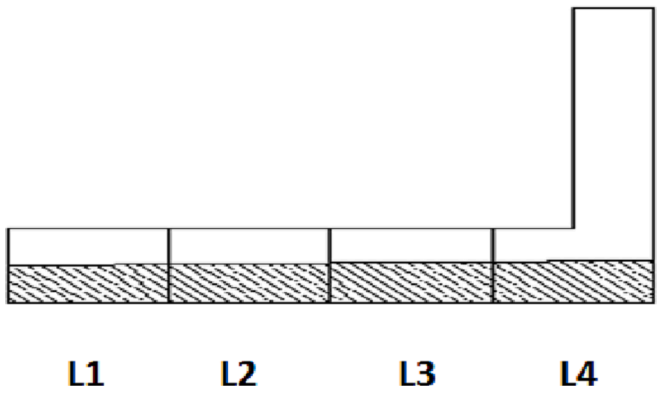


**Fig. 22.** Different sections in the L-box.

resistance, and compressive strength.

The standard stability tests of SCC measure stability at a laboratory scale and are not sensitive to concrete in workshop conditions or maintenance properties of concrete after implementation. In this part, to simulate workshop conditions in the laboratory and observe the effect of static and dynamic instability at actual scale, a beam with dimensions close to real-world dimensions (1.5 m length, 30 cm height, and 10 cm width) was constructed. Two types of self-compacting concrete (stable and unstable) were compared, investigating the parameters of apparent density, specific electrical resistance, and 28-day compressive strength to determine which concrete properties changed the most after implementation.

### 5.1. Experimental scheme

#### 5.1.1. Mix design

To compare the behavior of SCC with different stability levels during implementation, two different static stability levels were considered for the specimen. It should be noted that one of the designs used is the HS-S code which was used in previous chapters. For the other design, named the HS-S code, efforts were made to reach the same flow as the HS-S scheme while keeping the cement grade and w/c constant. However, this scheme was obtained by changing the gravel-to-sand ratio and the amount of additive compared to the HS-S scheme. The specifications of the two designs are listed in Table 7. Fig. 29 shows the effect of instability and stability during concreting.

#### 5.1.2. Experimental methods

In order to investigate the response of the concrete specimen with different stability levels, a wooden frame, shown in Fig. 30, was constructed with 1.5 m in length, 30 cm in height, and 10 cm in width.

After mixing concrete using the methods described in the previous chapters, the slump flow test was carried out to control the initial conditions. The casting was then applied slowly and from one side of the mold to flow freely in the form of flow and fill it without causing vibration. At the same time, the separation column was also filled. Six concrete cubes with 10×10×10 cm dimensions were sampled for each design, and the compressive strength of three cubes was measured after seven days and three after 28 days. After one day, the mold was opened, and the concrete was cured for a week between wet and plastic sacks. After a week, the concrete was divided into three sections in length and four sections in height. Each section was sampled by a diameter of 4 in. (10.16 cm) to provide a total of 12 samples for each design. Figs. 31 and 32 show the shapes of the templates after sampling, along with the numbering of the samples. It should be noted that the concrete was cast from the upper left corner of the image in both frameworks.

After opening the concrete mold, as indicated in Fig. 33, the beams did not differ significantly in the apparent aspect.

Four photos from different angles were taken from each sample to compare the distribution of aggregates on the surface of concrete specimens. Fig. 34(a) shows the surface of the beam with unstable concrete, while Fig. 34(b) is representative of a beam with stable concrete.

Then, the diameter, height, 10-day electrical resistance, saturated surface-dry weight (W_SSD), the weight of concrete immersed in water (according to instructions 97-ASTM C642 [62]), and compressive strength of the specimens were measured. In addition, the specific electrical resistance, apparent density, and 28-day compressive strength of 10×10×10 cm cubic specimens were obtained.

The specific electrical resistance is calculated using the relationship below:

$$\rho = \frac{R \times A}{L} \tag{1}$$

where $\rho$ is the specific resistance (kΩ-cm), $R$ is the calculated electrical resistance (kΩ), $A$ is the surface area of the sample ($cm^2$), and $L$ is the

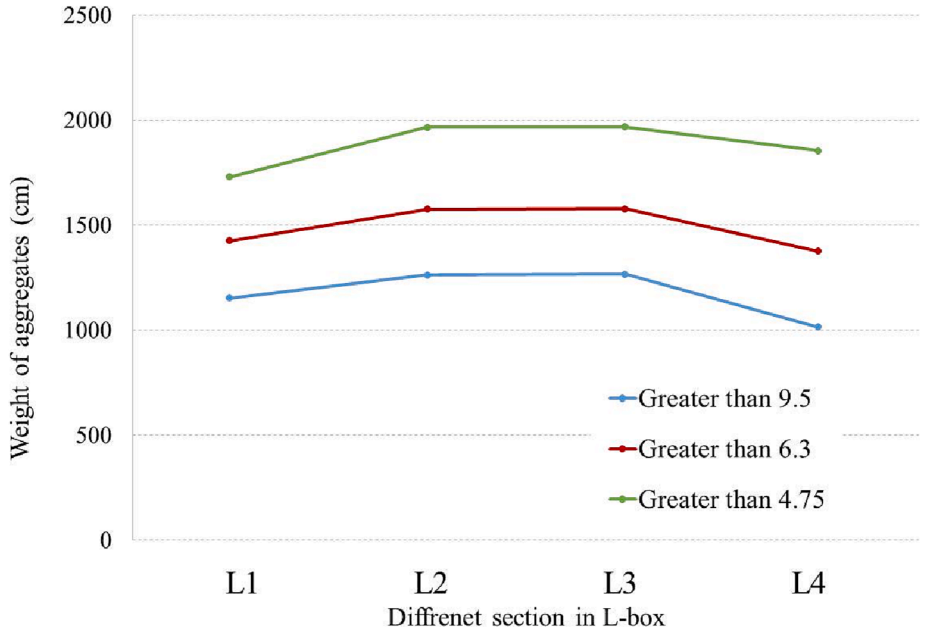


**Fig. 23.** The average weighted value of the aggregates per section of the L-box.

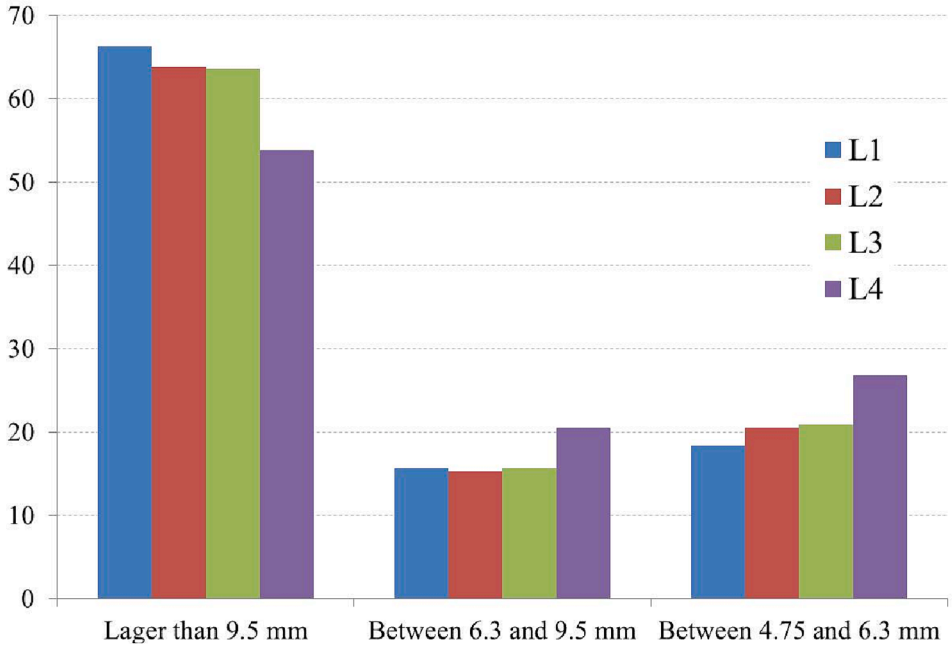


**Fig. 24.** The average weighted percentage of the aggregates per section of the L-box.

length of the sample (cm).

Moreover, to measure the electrical resistance of concrete under experimenal conditions, it should be noted that the concrete also exhibits capacitive properties in addition to electrical resistance. Therefore, to accurately measure the electrical resistance, the effect of this property should be eliminated. The device in the laboratory of the Construction Materials Institute (shown in Fig. 35) can remove the capacitive nature of concrete by changing the phase of an alternating current and extracting the actual electrical resistance of concrete [50].

Formula (2) is used to obtain the apparent density parameter:

$$Density = \frac{W_{SSd}}{W_{SSd} - W_{Immersed}} \quad (2)$$

where $W_{SSd}$ is the saturated surface-dry weight, and $W_{Immersed}$ is the immersed weight.

In this chapter, for simplicity in examining the variables, a factor called the coefficient of uniformity is defined as the coefficient for a variable to be closer to 100, which indicates that the examined part in that variable has a higher uniformity.

$$Uniformity\ Factor\ (\%) = \frac{R_{min}}{R_{max}} \times 100 \quad (3)$$

where $R_{min}$ and $R_{max}$ are the minimum and maximum obtained values for the variable, respectively.

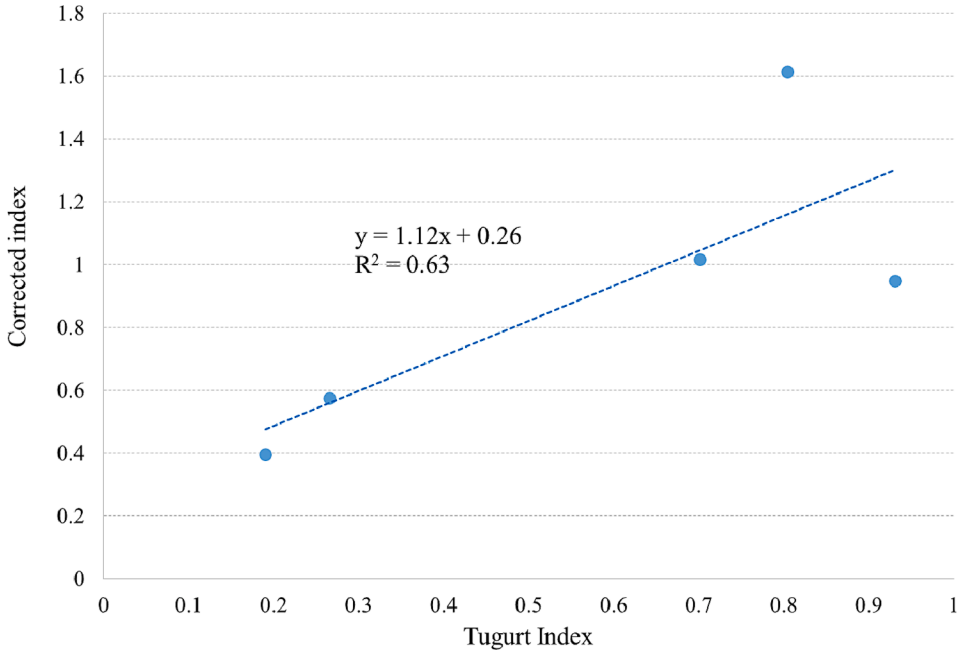


**Fig. 25.** Comparison of the separation index calculated by the Turgut index and the modified index.

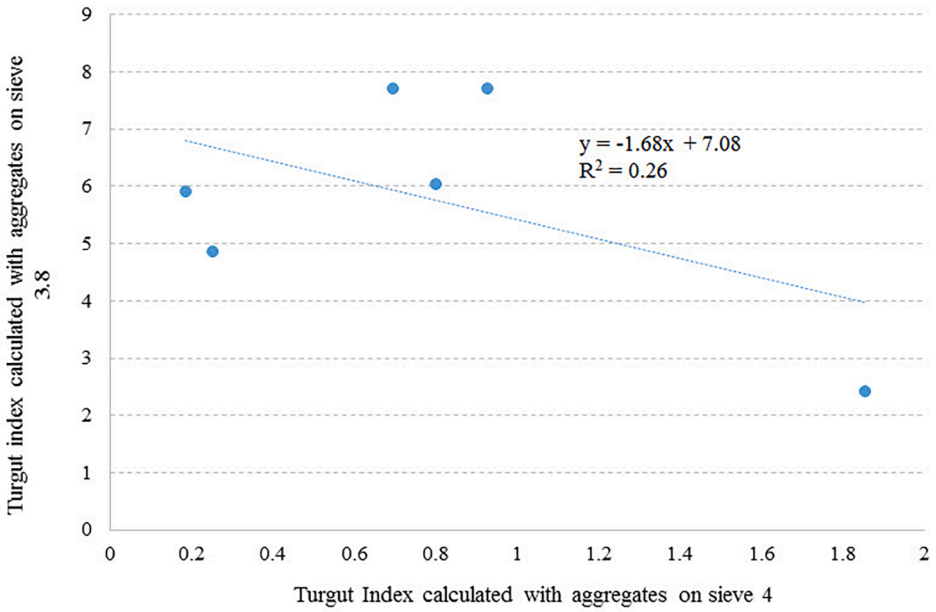


**Fig. 26.** Comparison between the Turgut indices computed with residual aggregates on sieve number 4 and the volume of the coarse aggregates bigger than 4.75 mm.

### *5.2. Provision of the results*

In summary, the results obtained for two test beams are shown in Tables 8 and 9.

During the investigation of the collected samples, the impact of static stability on the height of the beam was observed by vertically moving it along the upper and lower sections of the beam. In addition, the effect of dynamic stability on the specific electrical resistance, apparent density, and equivalent compressive strength in the beam's three upper, mid, and lower sections was examined. To better compare the variables investigated between the two beams, the mean values and the coefficient of change of these variables were calculated for the total samples taken from the beam and the four columns shown in Fig. 36. The results for the variables are depicted in the tables specified in the corresponding sections.

#### *5.2.1. Apparent density*

A comparison of the effect of static stability on two concrete beams with different stability on the apparent density of concrete is persented in Fig. 37.

As shown in the figure, in the unstable specimen (with the HS-U design code), the difference between the densities of different columns is more significant than that in the stable specimen (with the schema of the HS-S scheme). The farther the distance from the concrete casting, the greater the difference between the densities of the specimens. Therefore, it can be said that the static stability of concrete in horizontal sections for

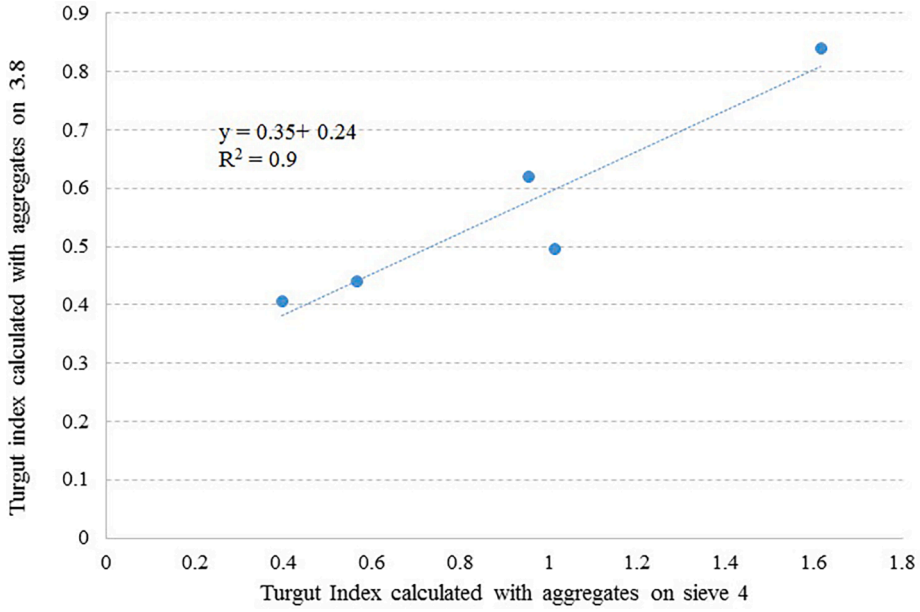


**Fig. 27.** Comparison of the modified index values for aggregates greater than 9.5 mm and the indices for the volume of the coarse aggregates greater than 4.75 mm.

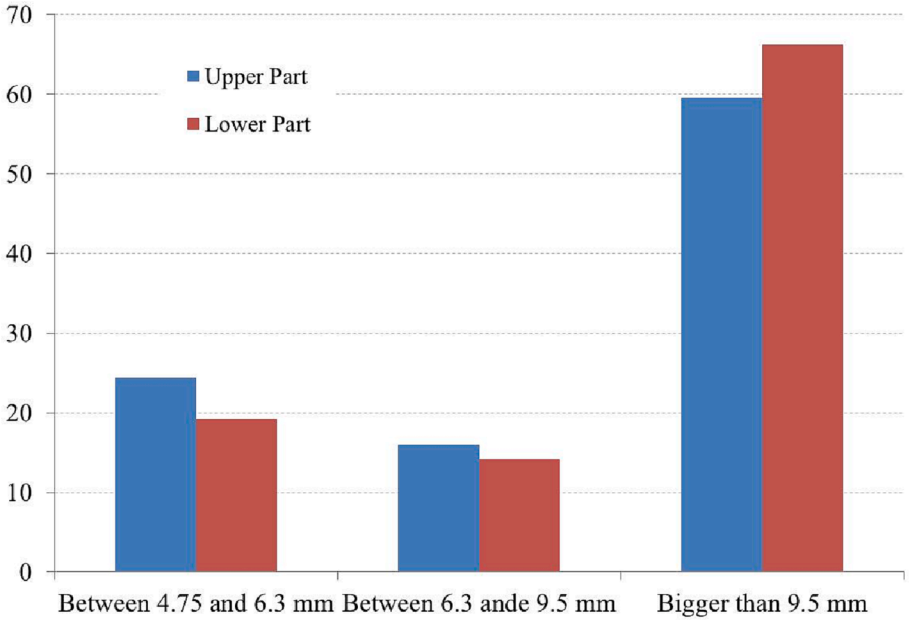


**Fig. 28.** The average percentile of the aggregate distribution of different sizes in the concrete of the upper and lower sections of the column separation test in 7 experiments.

**Table 7**
Mix design of the SCC in the beam simulation test.

| Scheme name | Target column index | Target slump (cm) | Water (kg/m$^3$) | Cement (kg/m$^3$) | Stone powder (kg/m$^3$) | w/c | Sand (kg/m$^3$) | Gravel (kg/m$^3$) | Super plasticizer (kg/m$^3$) |
|---|---|---|---|---|---|---|---|---|---|
| HS-S | 16.00 | 69.50 | 200.00 | 500.00 | 100.00 | 0.40 | 1236.00 | 412.00 | 3.75 |
| HS-U | 87.00 | 71.00 | 200.00 | 500.00 | 100.00 | 0.40 | 824.00 | 824.00 | 4.25 |

unstable concrete is more affected by the distance from the concrete casting point than that in stable concrete. Increasing the distance from the casting point results in a decrease in density compared to stable concrete.

Fig. 38 compares the effect of dynamic stability on the apparent density of two concrete beams with different stability levels. As seen in the figure, the stable concrete has managed to maintain the uniformity of its density by moving away from the point of concrete casting. However, the density of the unstable concrete is reduced as it moves away from the point of contact and cannot maintain its uniformity. This phenomenon is particularly noticeable when comparing the extreme points, which are the farthest points from the location of the concrete

(a) (b)

**Fig. 29.** Using different designs to observe the effect of instability in concreting in the specimens with (a) unstable concrete, and (b) stable concrete.

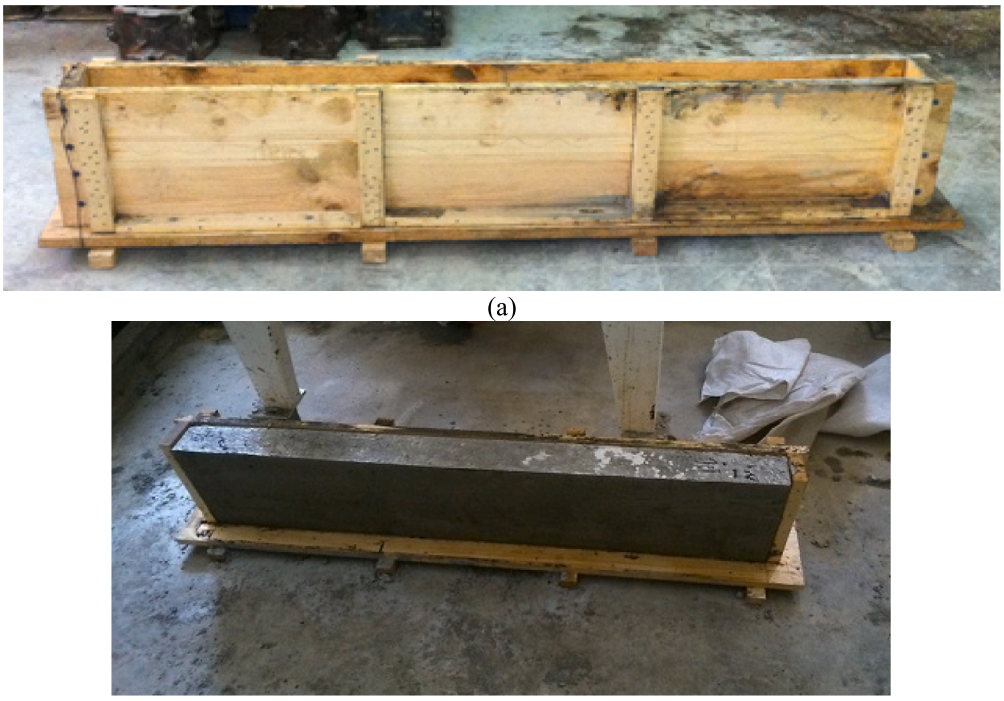

(a)

(b)

**Fig. 30.** Experimental setup of (a) wooden frame used in the beam simulation test, and (b) concrete beam before sampling.

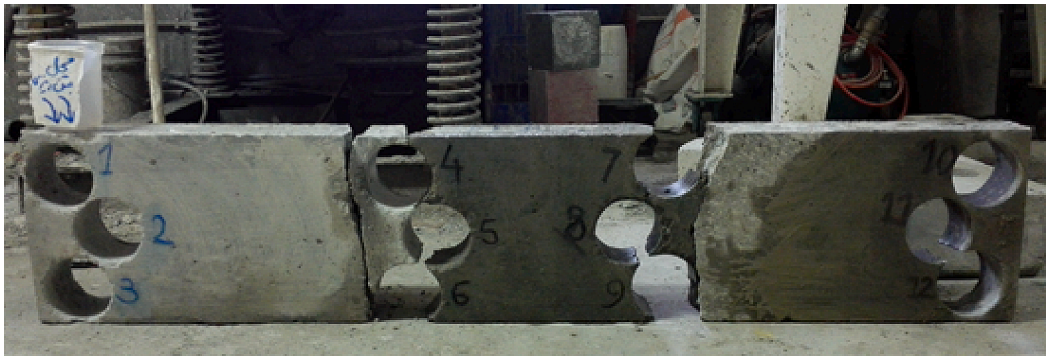


**Fig. 31.** HS-S scheme after sampling.

**Fig. 32.** LS-S scheme after sampling.

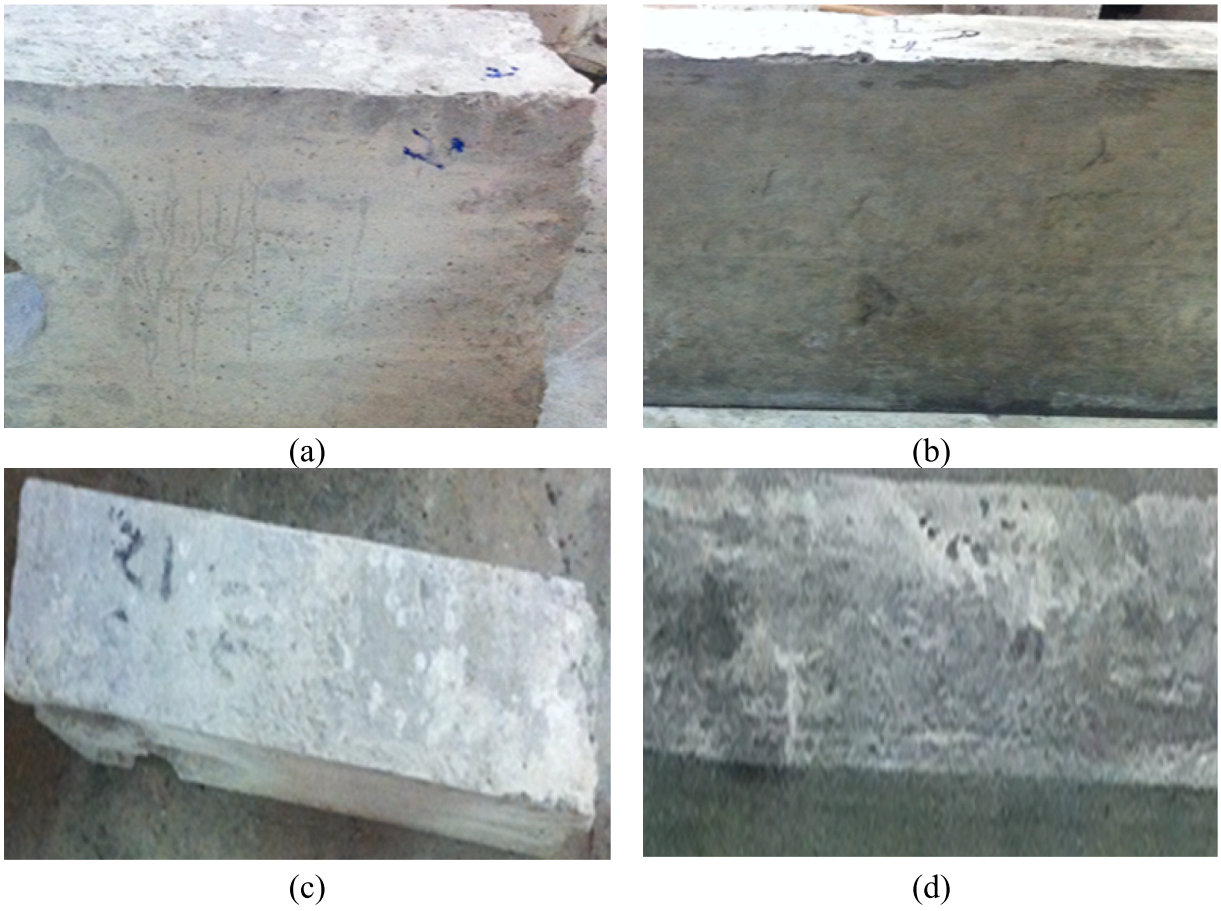


**Fig. 33.** Examination of the appearance of the lateral surface of the beams made with (a) stable concrete and (b) unstable concrete. Examination of the appearance of the upper surface of the beams made with (c) stable concrete and (d) unstable concrete.

casting.

Table 10 presents the mean values, variation coefficient, and uniformity coefficient for calculating the apparent density of all rows, columns, and the entire beam made from stable and unstable concrete. As can be seen, the apparent density in all rows, columns, and the full beam with stable concrete has less variation and a higher uniformity coefficient compared to the beam with unstable concrete, indicating a smoother distribution of density in the volume of the beam with stable concrete. As observed in the table, the apparent density decreases by 3% for the beam with stable concrete, while the amount of this decrease in the beam with unstable concrete is 8%.

To draw contours of density, electrical resistance and compressive strength, different samples were obtained by core drilling in beams. Then, the desired parameters were obtained in the core samples experimentally, and according to the obtained results, different contours were drawn along the length of the beam. The density contour for two beams is presented in Fig. 39. The figure clearly demonstrates that the density of stable concrete is much more uniform than unstable concrete throughout the beam's volume. Moreover, the density difference in unstable concrete increases with the distance from the casting point. Generally, the mass in beams with stable concrete is evenly distributed within the beam volume, whereas in unstable concrete, more mass is concentrated in the concrete segments and dispersed throughout the beam. Nevertheless, the average density of the two beams is nearly

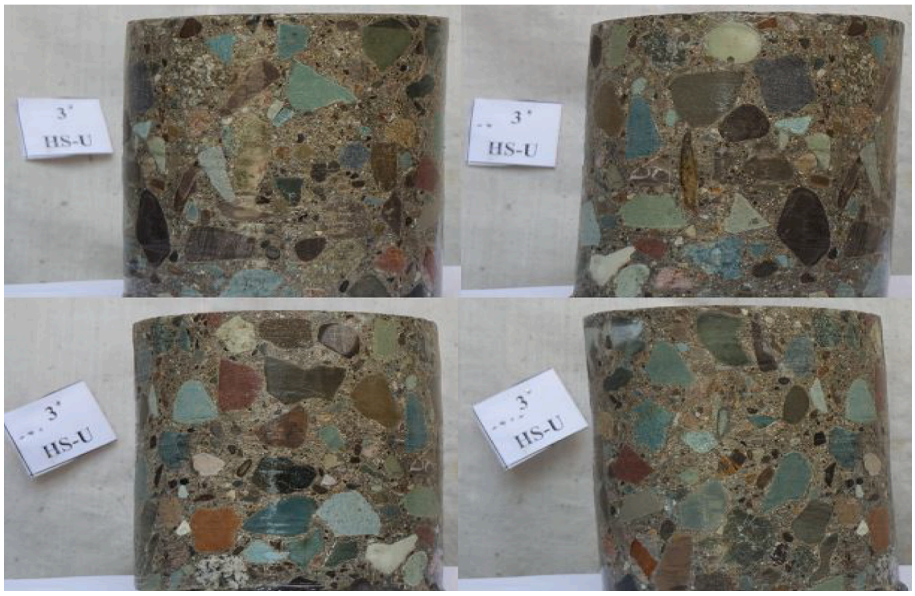


(a)

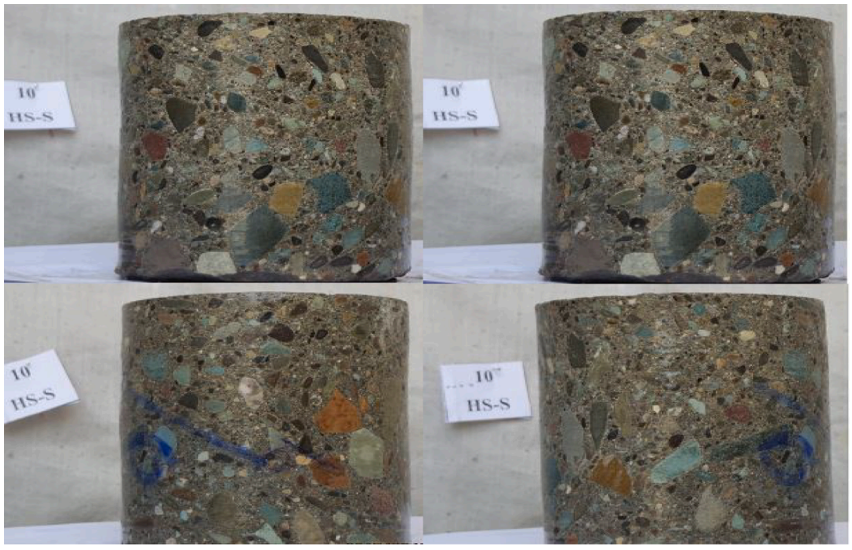


(b)

**Fig. 34.** Distribution of the aggregates on the surface of concrete specimens: (a) HS-S specimens and (b) HS-U specimens.

equal; there is a density reduction of approximately 120 Kg/m$^3$, indicating the lack of uniformity in the beam with unstable concrete.

*5.2.2. Specific electrical resistance*

The comparison of the effect of static stability of two concrete beams with different stability on the concrete resistivity is carried out in Fig. 40.

In general, unstable concrete specimens have less specific electrical resistance than stable concrete specimens. In addition, the difference between the specific electrical resistance of specimens made with unstable concrete in different columns increases when going further from the casting point. This difference is much lower in the specimens made with stable concrete.

Fig. 41 compares dynamic stability's effect on the specific electrical resistivity in two concrete beams with different stability.

As shown in the figure, stable concrete maintains uniformity in its characteristic electrical resistance, whereas unstable concrete exhibits a reduction in its specific electrical resistance and cannot maintain uniformity. Moreover, it should be noted that unstable concrete typically has a lower specific electrical resistance than stable concrete.

Table 11 presents the mean values, coefficient of variation, and uniformity coefficient for specific electrical resistivity of all rows and columns and the entire beam made of stable and unstable concrete. As can be seen, the coefficient of variation and uniformity coefficient for this variable are generally higher than those for the density variable. However, these values are higher for the stable concrete beams compared to the unstable concrete beams. The coefficient of uniformity of resistivity in the full beam with unstable concrete is 42%, indicating that the resistivity distribution in this beam is not uniform, and the electrical resistivity drop is approximately 58% in the entire beam. On the other hand, the decrease in electrical resistivity in the stable concrete beam is 21%.

In order to demonstrate the distribution of specific electrical resistivity in the beam volume, the contour of specific electrical resistivity is plotted for two beams in Fig. 42. The stable concrete has a more uniform distribution in its volume. In addition, the average specific

**Fig. 35.** The device in the laboratory of the construction materials institute.

electrical resistivity in the volume of the beam made with stable concrete is also higher compared to the beam made with unstable concrete, which results in a better utility of the structure.

### 5.2.3. Compressive strength

The comparison of the effect of static stability on the equivalent compressive strength of two concrete beams with different stability of 10×10 ×10 cm cubic specimen is depicted in Fig. 43.

A decreasing trend in compressive strength can be observed in the beam made of stable concrete. However, in the beam made of unstable concrete, a specific trend is not apparent in different rows, and a consistent pattern cannot be observed for the entire beam. Overall, the compressive strength values in the beam with stable concrete are higher than those with unstable concrete. It is worth noting that the cement grade and the w/c are similar in both designs.

Fig. 44 compares the effect of dynamic stability on the equivalent compressive strength in two concrete beams with different stabilities.

As shown in Fig. 44, the changes in compressive strength in the lower half of both beams fluctuate as the distance from the casting point increases, making it difficult to predict the trend. For example, in the beam with stable concrete, the compressive strength increases as the distance from the casting point increases, but it remains almost constant in the first and third columns and decreases drastically in the fourth column. However, no particular disorder was observed in the investigation of apparent density and specific electrical resistivity for stable concrete. Maintaining the compressive strength of areas far from the casting point can be challenging. Therefore, it is recommended to restrict the distance between casting points to control the reduction of compressive strength in the surrounding points far from the casting point.

Table 12 presents the mean values, coefficient of variation, and calculated uniformity coefficient for the equivalent compressive strength of all rows and columns and the entire beam made of stable and unstable concrete. As can be seen, the beam made of stable concrete is generally less uniform in terms of the coefficient of variation and uniformity coefficient compared to the beam made of unstable concrete. However, the average compressive strength of the stable concrete beam is higher than that of the unstable concrete beam. One of the reasons for this difference could be errors in conducting the test due to the

**Table 8**
Summary of the results of the tests performed on the HS-S mixture.

| Sample number | 1 | 2 | 3 | 4 | 5 | 6 | 7 | 8 | 9 | 10 | 11 | 12 |
|---|---|---|---|---|---|---|---|---|---|---|---|---|
| Apparent density (g/cm$^3$) | 2.32 | 2.31 | 2.30 | 2.35 | 2.32 | 2.33 | 2.34 | 2.33 | 2.32 | 2.31 | 2.29 | 3.32 |
| Specific electrical resistance (kΩ-cm) | 4.16 | 4.07 | 4.02 | 3.80 | 3.51 | 3.96 | 4.25 | 4.21 | 3.91 | 3.47 | 3.99 | 4.39 |
| Equivalent compressive strength (MPa) | 43.37 | 39.02 | 40.35 | 37.99 | 36.00 | 40.11 | 41.02 | 34.59 | 34.08 | 39.38 | 37.00 | 31.05 |

**Table 9**
Summary of the results of the tests performed on the HS-U mixture.

| Sample number | 1 | 2 | 3 | 4 | 5 | 6 | 7 | 8 | 9 | 10 | 11 | 12 |
|---|---|---|---|---|---|---|---|---|---|---|---|---|
| Apparent density (g/cm$^3$) | 2.38 | 2.36 | 2.38 | 2.37 | 2.34 | 2.37 | 2.35 | 2.36 | 2.35 | 2.19 | 2.26 | 2.26 |
| Specific electrical resistance (kΩ-cm) | 3.17 | 3.24 | 3.35 | 3.48 | 2.94 | 3.80 | 2.86 | 3.07 | 2.52 | 1.41 | 2.46 | 2.18 |
| Equivalent compressive strength (MPa) | 33.25 | 38.17 | 35.45 | 33.48 | 31.78 | 33.18 | 31.07 | 35.15 | 33.89 | 33.90 | 36.55 | 37.28 |

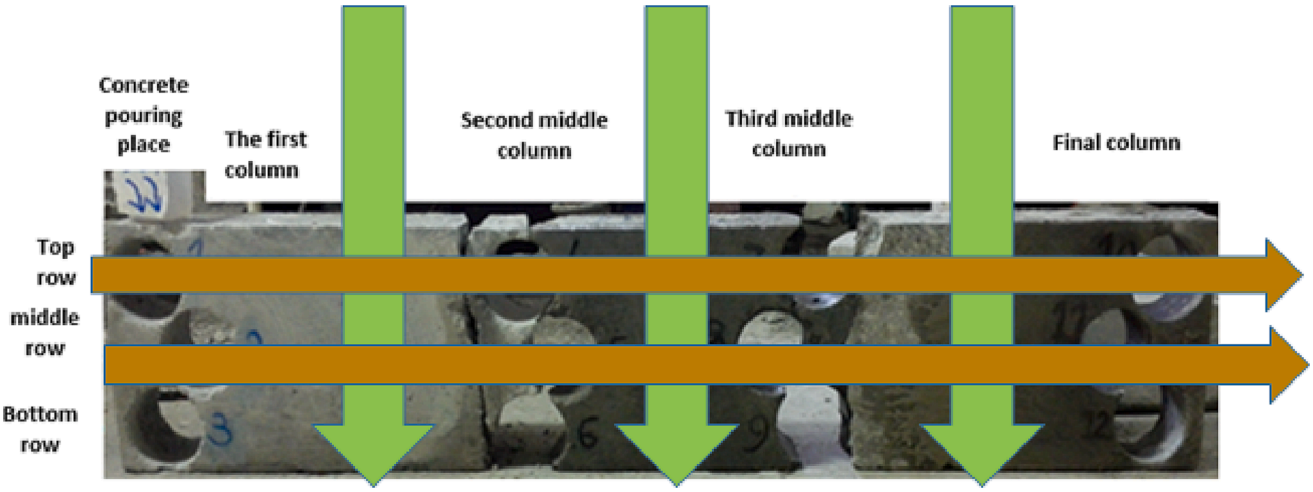


**Fig. 36.** The names of columns and beam rows.

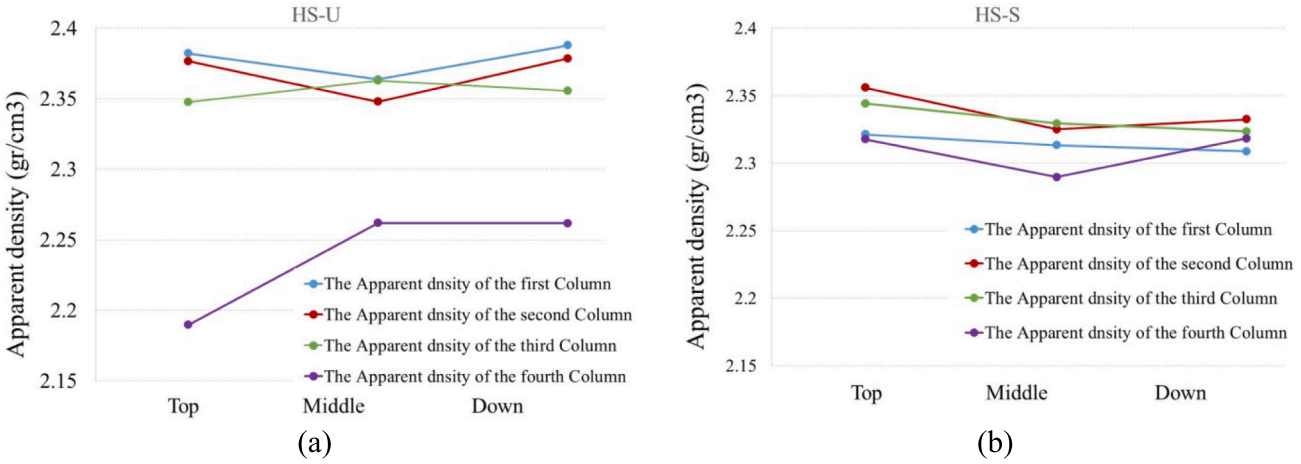


**Fig. 37.** Comparison of the effect of the static stability on the apparent density of two concrete specimens (a) unstable concrete and (b) stable concrete.

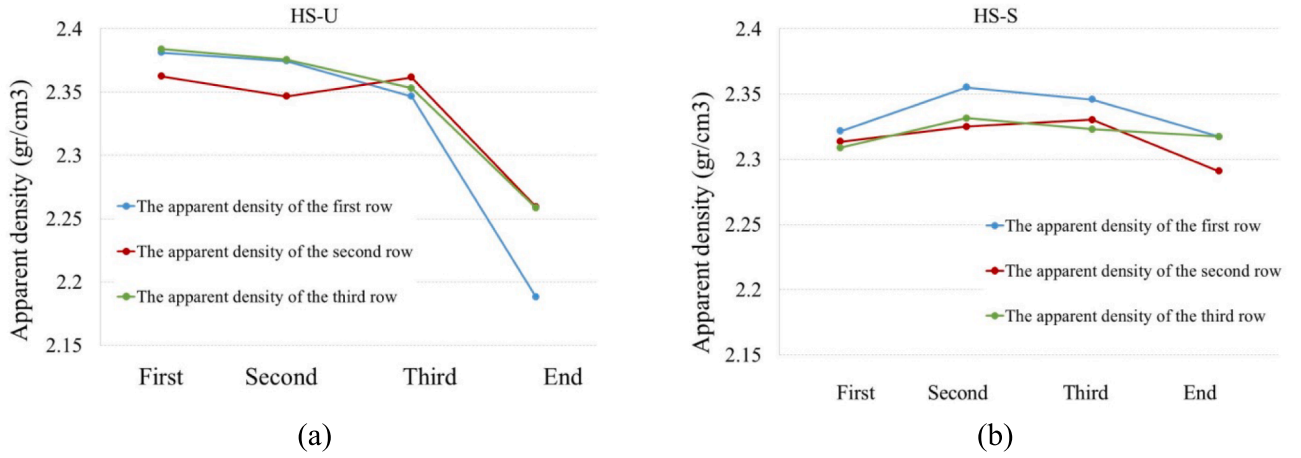


**Fig. 38.** Comparison of the effect of the dynamic stability on the apparent density of two concrete specimens (a) unstable concrete and (b) stable concrete.

**Table 10**
The mean values, variation coefficient, and uniformity coefficient for calculating the apparent density.

| | Upper Row | Middle Row | Lower Row | First Column | Second Column | Third Row | Last Row | Full Beam |
|---|---|---|---|---|---|---|---|---|
| Mean in concrete beam HS-S | 2.33 | 2.31 | 2.31 | 2.31 | 2.34 | 2.33 | 2.31 | 2.32 |
| Mean in concrete beam HS-U | 2.32 | 2.33 | 2.34 | 2.37 | 2.37 | 2.35 | 2.24 | 2.32 |
| Variation coefficient in concrete beam HS-S (%) | 0.68 | 0.76 | 0.26 | 0.25 | 0.67 | 0.67 | 0.69 | 0.72 |
| Variation coefficient in concrete beam HS-U (%) | 3.54 | 1.92 | 2.16 | 0.52 | 0.71 | 0.32 | 1.83 | 2.65 |
| Uniformity coefficient in concrete beam HS-S (%) | 98.00 | 98.00 | 99.00 | 100.00 | 99.00 | 99.00 | 99.00 | 97.00 |
| Uniformity coefficient in concrete beam HS-S (%) | 92.00 | 96.00 | 95.00 | 99.00 | 99.00 | 99.00 | 99.00 | 92.00 |

heterogeneity of the concrete surface after drilling for sample collection. Although stable concrete beams appear less homogeneous than unstable ones, with the same cement content and w/c, unstable concrete has a higher compressive strength. In beams made of stable concrete, the loss of resistance in the entire beam is 28%, while the decrease in the beam made of unstable concrete is 19%. However, the mean compressive strength in beams made of unstable concrete is 9% less than the value of this variable in beams made of stable concrete. It should be noted that in the beam made of stable concrete, if we consider the first 1 m length instead of the 1.5 m length of the beam, the uniformity coefficient in the entire beam increases from 72% to 79%, which indicates the necessity of restricting the distances where the casting is performed.

The equivalent compressive strength contour for both beams is plotted in Fig. 45. Although the distribution of this variable in the whole volume of the unstable concrete beam is more heterogeneous than that of the stable concrete beam, the equivalent compressive strength values in the beam with stable concrete are higher than those of unstable concrete.

On the other hand, it is observed that the resistance decreases with increasing distance from the casting point so that the furthest corner of this point has the lowest compressive strength (about a 30% reduction compared to the casting point). However, the middle part has the lowest compressive strength in beams with unstable concrete. The higher compressive strength of the furthest parts from the casting point than the middle liners can be attributed to more cement mortar in the region due to dynamic separation. The summary of the results related to the simulation test with the beam shape is given in Table 13.

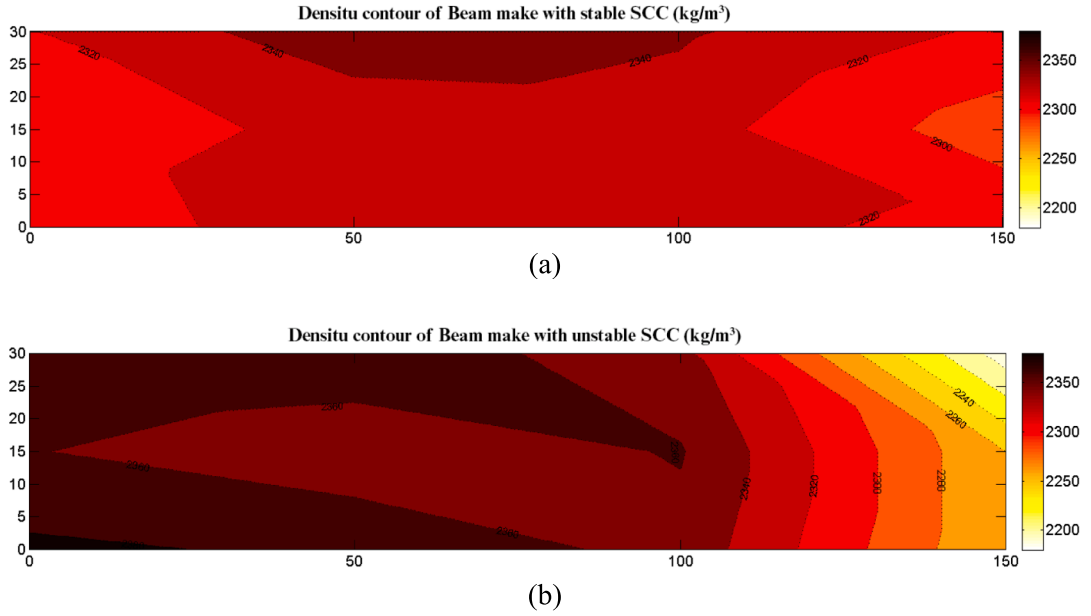


**Fig. 39.** The distribution of the concrete density contour in the beam with (a) stable concrete, and (b) unstable concrete.

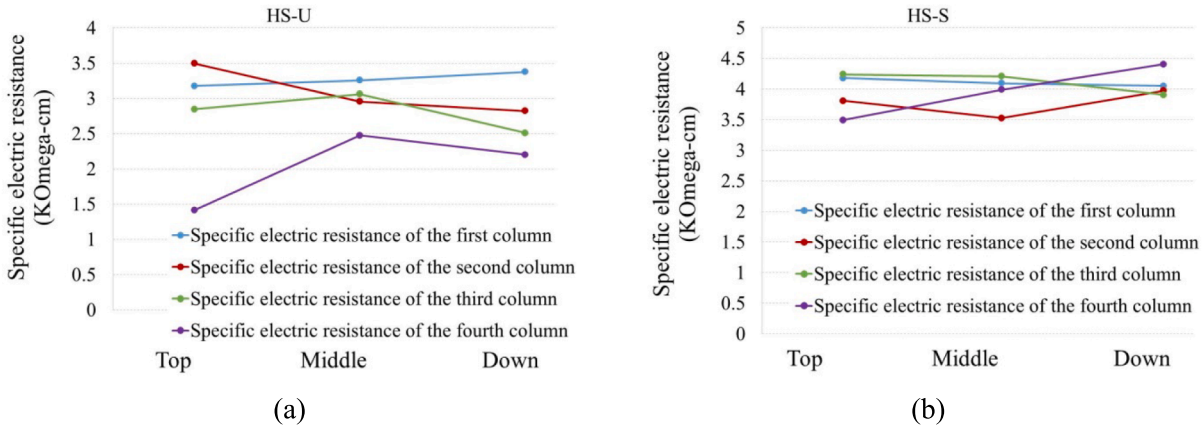


**Fig. 40.** Comparison of the effect of static stability on the specific electrical resistivity of two beams with (a) stable concrete and (b) unstable concrete.

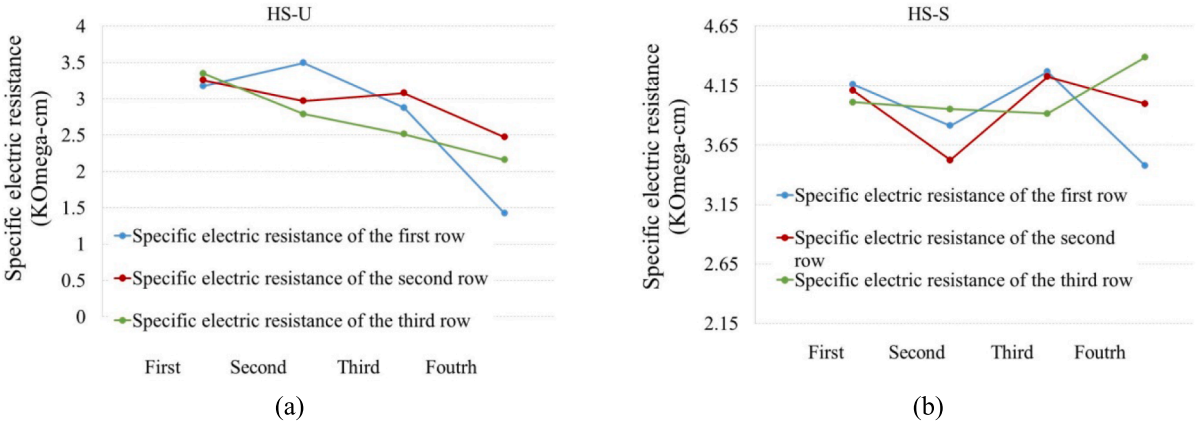


**Fig. 41.** Comparison of the effect of dynamic stability on the specific electrical resistivity of two beams with (a) unstable concrete and (b) stable concrete.

## 6. Results

All the aforementioned tests, except for the J-ring and L-box indices, exhibit good repeatability of less than 5%. In the case of the measured variables in the J-ring test, the difference between the opening radius and the slump flow displays good repeatability compared to other flow

**Table 11**
The mean values, variation coefficient, and uniformity coefficient to calculate the specific electrical resistivity.

| | Upper Row | Middle Row | Lower Row | First Column | Second Column | Third Row | Last Row | Full Beam |
|---|---|---|---|---|---|---|---|---|
| Mean in concrete beam HS-S | 3.92 | 3.95 | 4.07 | 4.09 | 3.76 | 4.13 | 3.95 | 3.98 |
| Mean in concrete beam HS-U | 2.46 | 2.93 | 2.72 | 3.26 | 2.71 | 2.82 | 2.02 | 2.70 |
| Variation coefficient in concrete beam HS-S (%) | 8.25 | 7.44 | 5.32 | 1.69 | 6.06 | 4.50 | 11.74 | 7.04 |
| Variation coefficient in concrete beam HS-U (%) | 24.88 | 9.02 | 10.10 | 2.90 | 10.93 | 9.74 | 26.76 | 20.20 |
| Uniformity coefficient in concrete beam HS-S (%) | 82.00 | 83.00 | 89.00 | 97.00 | 89.00 | 92.00 | 79.00 | 79.00 |
| Uniformity coefficient in concrete beam HS-S (%) | 45.00 | 76.00 | 65.00 | 94.00 | 81.00 | 82.00 | 58.00 | 42.00 |

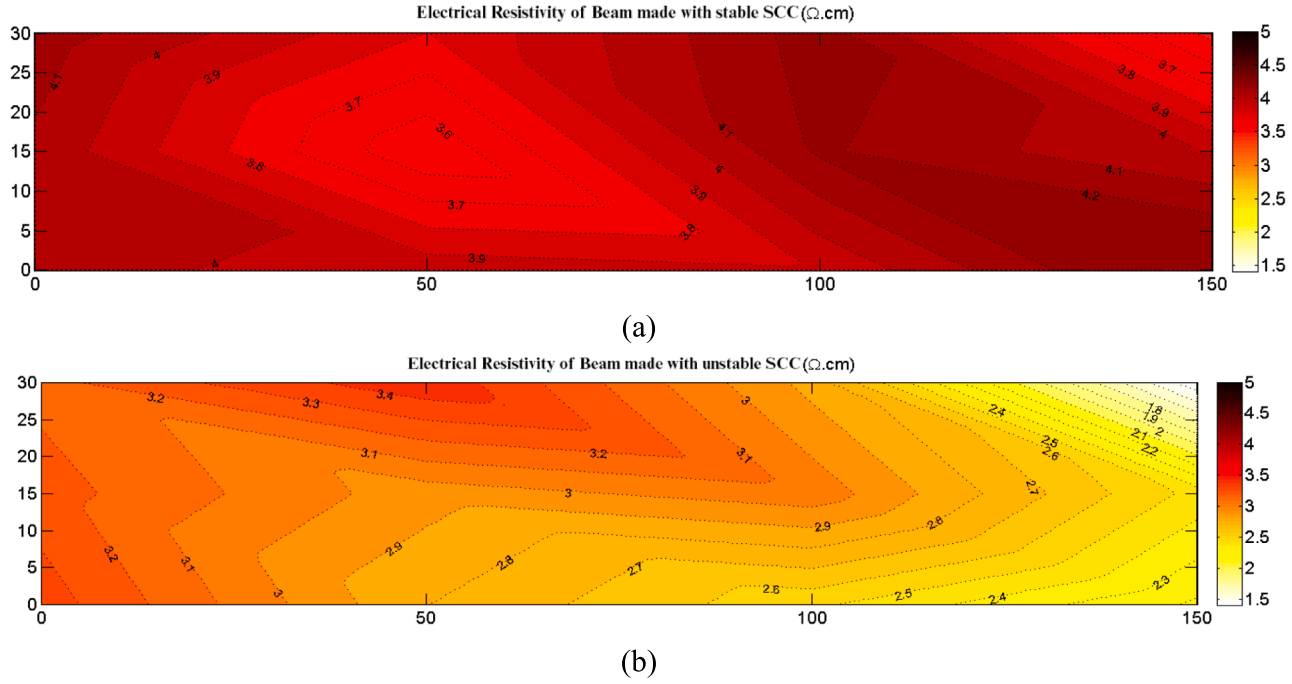


**Fig. 42.** The specific electrical resistivity contour of the beams made with (a) stable concrete, and (b) unstable concrete.

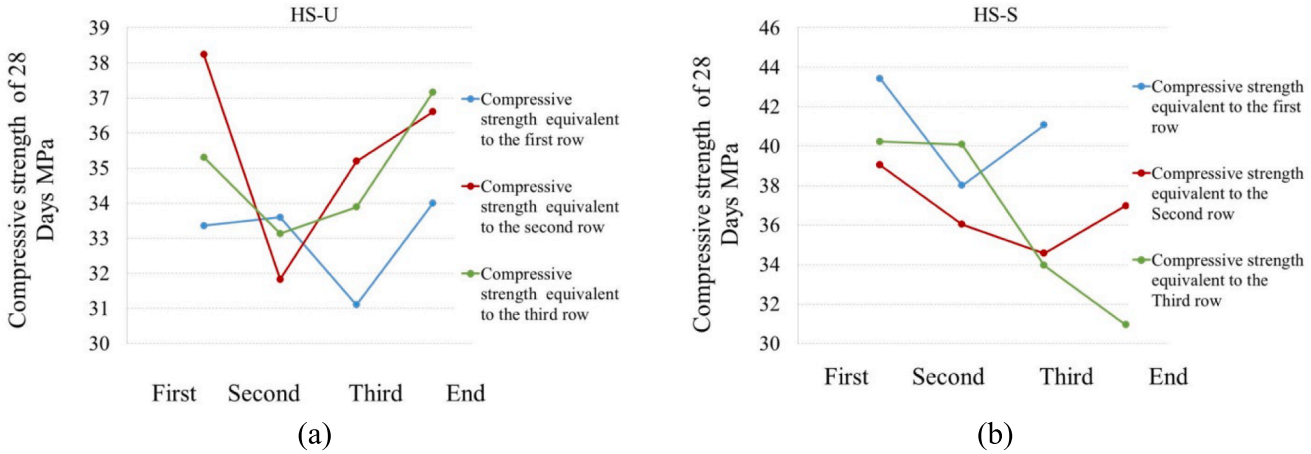


**Fig. 43.** The Comparison of the effect of static stability on the equivalent compressive strength of two concrete beams with (a) unstable concrete, and (b) stable concrete.

conditions. Furthermore, the opening radius variable demonstrates good repeatability with the flow rate in concrete with a slump flow of 60. However, calculating the difference between the height of concrete inside and outside the ring does not exhibit accurate repeatability. The modified L-box index does not display good repeatability in terms of appearance, but based on the observations made in this research, it is possible to determine or reject concrete stability. Similarly, the blocking index of the L-box is also not repeatable.

All experiments conducted between the two design schemes, except for the differences inside and outside the J-ring and the rocking system, are suitable for measurement using SRM. They are capable of recognizing the difference between two different flow mixtures and stability

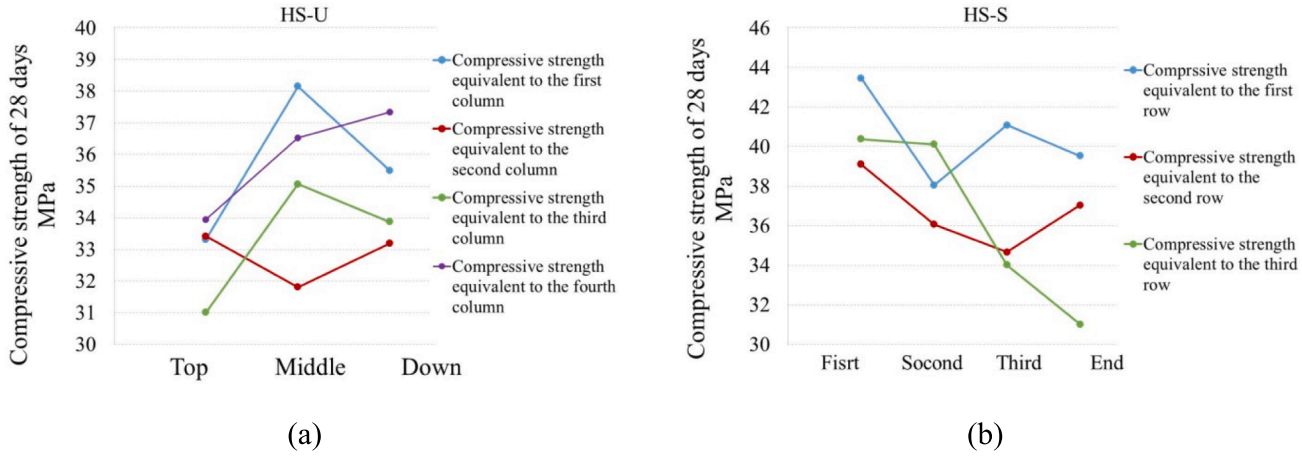


**Fig. 44.** Comparison of the effect of dynamic stability on the equivalent compressive strength in two concrete beams with (a) unstable concrete and (b) stable concrete.

**Table 12**
The mean values, variation coefficient, and uniformity coefficient to calculate the equivalent compressive strength.

| | Upper Row | Middle Row | Lower Row | First Column | Second Column | Third Row | Last Row | Full Beam |
|---|---|---|---|---|---|---|---|---|
| Mean in concrete beam HS-S | 40.44 | 36.25 | 36.40 | 40.92 | 38.04 | 36.57 | 35.81 | 37.83 |
| Mean in concrete beam HS-U | 32.93 | 35.41 | 34.95 | 35.63 | 32.81 | 33.73 | 35.91 | 34.43 |
| Variation coefficient in concrete beam HS-S (%) | 3.30 | 2.91 | 10.51 | 5.45 | 5.41 | 10.58 | 11.98 | 9.12 |
| Variation coefficient in concrete beam HS-U (%) | 3.79 | 5.80 | 5.13 | 6.92 | 2.77 | 6.26 | 4.96 | 6.25 |
| Uniformity coefficient in concrete beam HS-S (%) | 88.00 | 89.00 | 77.00 | 90.00 | 90.00 | 83.00 | 79.00 | 72.00 |
| Uniformity coefficient in concrete beam HS-S (%) | 92.00 | 83.00 | 89.00 | 87.00 | 95.00 | 88.00 | 91.00 | 81.00 |

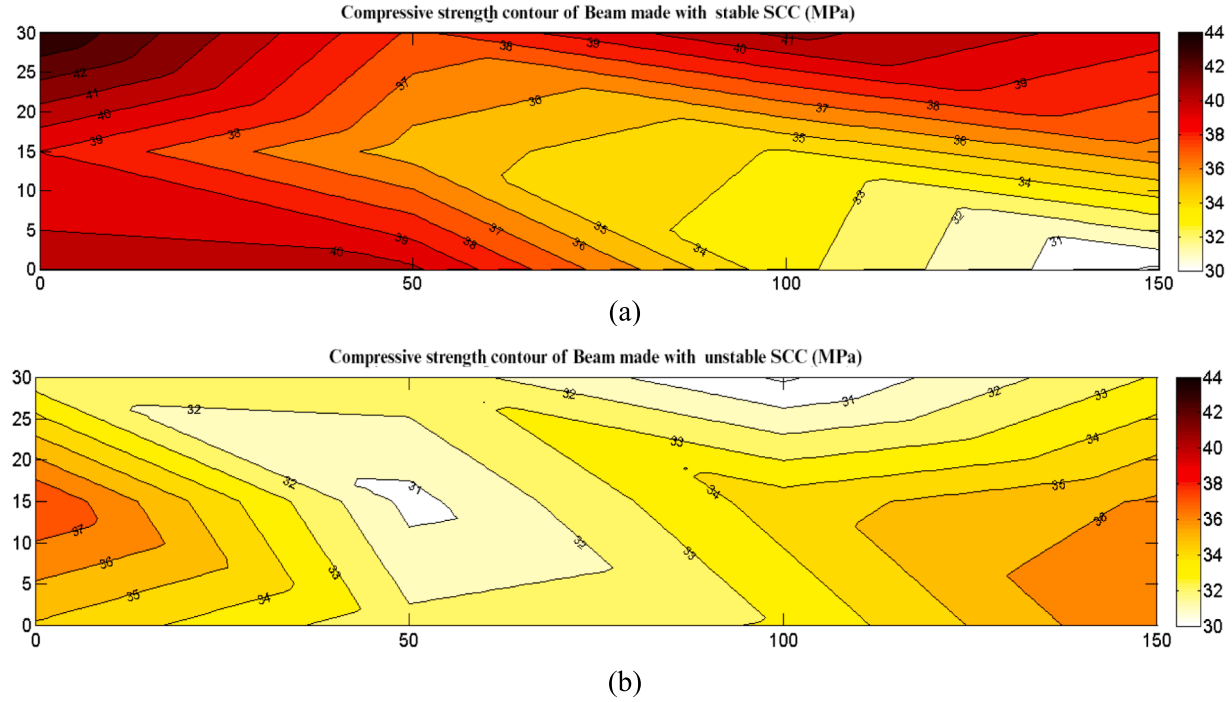


**Fig. 45.** The equivalent compressive strength contour of the beams made with (a) stable concrete, and (b) unstable concrete.

values. However, the blocking index of the L-box test does not perform well in detecting the difference between two mixtures with the same flow value and stability values. Nonetheless, it performs well in detecting the difference between two mixtures with different flow values.

The reproducibility of the experiments decreases as the concrete flow increases. However, tests that exhibit acceptable reproducibility, except for the opening radius of the J-ring experiment with increased flow, will remain highly repeatable with less than 5% variability.

This research introduces three penetration tests: a probe, a modified

**Table 13**
Summary of the results of samples obtained from beams.

| | Average in stable beam | Average in unstable beam | Coefficient of uniformity in stable beam | Coefficient of uniformity in unstable beam |
|---|---|---|---|---|
| Apparent density | 2.32 g/cm$^3$ | 2.32 g/cm$^3$ | 97% | 92% |
| Specific electrical resistance | 3.98 kΩ-cm | 2.70 kΩ-cm | 79% | 42% |
| Standard compressive strength | 36.03 MPa | 32.79 MPa | 72% | 81% |

probe, and an instability estimation approach for concrete, which were performed on the top surface of the concrete. All three tests exhibit a linear relationship with high correlation (with correlation coefficients of more than 0.72) and can be used interchangeably. The relationship between these three experiments with the separation column index (as the determinant of the static separation value) was also investigated, showing a linear relationship with a correlation coefficient of 0.76 between the separation column and the probe. This indicates the possibility of using surface infiltration experiments instead of separation column experiments. Due to its simplicity in the test apparatus's fabrication and symmetry in the apparatus, we recommend using the modified probe instead of other surface infiltration experiments. For estimating the static separation, the amount of 6 mm for the modified probe (equivalent to the separation column index of 10, which is the standard of the 237 committees of the American Concrete society for instability) is determined to confirm the critical limit of the stability of concrete.

The modified L-box index, which was developed to measure dynamic stability, has a high correlation coefficient with surface infiltration experiments. For example, the correlation coefficient of this index with the penetration test is 0.75. It was also found that the separation column index had a correlation coefficient of 0.68. For this reason, the dynamic instability measured by this index (measured without introducing external energy to the instrument) is a function of static stability. When comparing the modified L-box index with the separation column experiment, it was observed that the modified L-box requires less concrete volume (12 L compared to 20 L needed for the separation column). After pouring concrete, the test can be performed quickly, and the required sections can be sifted. On the other hand, the separation column test needs 15 to 20 min after concrete casting. The volume and complexity of calculations required to calculate the modified L-box index are more significant than the calculation of the separation column index, which is obtained only by inputting numbers into a formula. In general, the decision on which experiment to use can be made by evaluating the advantages and disadvantages of each and conducting a feasibility study. Due to the linear and direct relationship between the modified L-box index and static stability tests, it can be used interchangeably with the separation probe test. The critical value of the modified probe penetration corresponding to the modified L-box index is equal to 1 cm, which is the critical value proposed for dynamic stability.

The blocking ratio of the L-box experiment with the modified L-box index, the separation column experiment index, the tilt box, and surface penetration tests is not particularly relevant, and measuring this coefficient is not recommended for determining concrete stability.

The stability measurement tests did not observe a significant difference in the variables of the concrete openings between those with no limit and the height difference inside and outside the J-ring test loop. As a result, this experiment is not recommended for estimating instability.

The rocking experiment, which is used to estimate the dynamic instability, does not have a particular relationship with the modified L-box experiment. The penetration index of this experiment for concrete with constant flow and grade of cement has a linear correlation coefficient of 0.92 with the separation column index. However, the results of the rocking experiment are not directly related to the results of static stability tests. The critical value of 1.2 cm for the initial penetration variable (P1) can be used as a threshold for static stability based on the similarity between the P1 and surface infiltration tests. There is also a linear relationship between P1 and the modified probe test, with a correlation coefficient of 0.73. If the dynamic stability of concrete during the application of external energy, such as pumping, needs to be determined, a rocking experiment can be used to estimate dynamic instability. Moreover, the P1 test, which has a critical value of 1.2 cm, can be used to estimate static instability.

The dynamical instability measured by the modified L-box experiments and the tilt box is different. According to the results, the dynamic stability of concrete against the impact and application of external energy can be attributed to the static stability and grade of cement. In contrast, its dynamic stability regarding its flow due to its weight will be a function of the static stability of concrete.

Instead of performing the costly and time-consuming separation column test to confirm or disprove the static stability of a specimen, a more affordable and faster experiment, like the modified probe test, can be used. This test has a critical value of 6 mm.

Comparing the apparent density and specific electrical resistance, it is evident that the beam with stable concrete has a more uniform distribution than the beam with unstable concrete. The coefficient of variation for the apparent density in the stable concrete beam is 0.72%, while it is 2.65% in the unstable concrete beam. Regarding specific electrical resistance, the stable concrete beam has an amount of 7.04%, while the unstable concrete beam has 20.2%.

When considering the 28-day compressive strength variable, the stable concrete beam shows a higher variation of 9.12% compared to the unstable concrete beam, which correlates with 6.25%. However, the mean compressive strength value in the stable concrete beam is 38.83 MPa, which is higher than the mean compressive strength in the unstable concrete beam, reported as 9%.

In the study of compressive strength values in beams, it was observed that the value of this variable in the stable concrete beam decreases as the distance from the casting point increases. For example, at a distance of 1.5 m from the casting point, the compressive strength value decreases by 30%. Therefore, it is recommended to limit the distance between casting points during execution. On the other hand, in the unstable concrete beam, the compressive strength value decreases as the distance from the starting point increases. This can be attributed to the heterogeneous movement of concrete along the route of filling the beam due to the presence of more cement in areas far from the casting point.

In the three investigated variables, instability had the highest impact on the specific electrical resistivity, resulting in a 58% decrease in the beam with unstable concrete compared to a 21% reduction in the beam with stable concrete. In addition, the apparent density decreased by 3%, and the compressive strength decreased by 28% in the volume of the beam with stable concrete, while in the beam with unstable concrete, the apparent density increased by 8%, and the compressive strength decreased by 19%.

The ratio of the mean value of the specific electrical resistivity in the beam with stable concrete is 32% less than that of the beam with unstable concrete. In the compressive strength variable study, the beam with unstable concrete showed 9% less resistance than that with stable concrete.

As the length of the beam with stable concrete is reduced from 1.5 m to 1 m, the uniformity coefficient increases by 9%, indicating the necessity of controlling the distance of the casting points to control the value of the compressive strength reduction in the beam.

It is suggested to repeat the tests on specimens taken from longer molds and compare the results. The use of reinforced formwork is recommended to examine the behavior between the reinforcements and concrete, as well as the corrosion potential of the reinforcements in two

beams with different stability levels.

## 7. Conclusion

In this study, the effectiveness of stability measurement tests for self-compacting concrete was compared by examining their repeatability and measurability properties. Tests were conducted on two types of concrete with different fluidity and stability, and the relationship between the tests was investigated. The possibility of using simpler and more cost-effective tests instead of harder and more expensive ones was also explored. Finally, the effects of instability on beam execution were tested. The results of the study can be summarized as follows:

The stability of fresh SCC means the ability of concrete to maintain homogeneity and resistance against the separation of each component during mixing, wetting, and drying. Instability may occur in various forms, such as separation, bleeding, blockage, and settling particles.

Investigation of the repeatability of the experiments showed that except for the J-ring test indices and the blocking index, the other test results have good repeatability of 5%, which makes them acceptable.

The study investigated the capability of various tests to distinguish between two mixtures with different flow and stability. It was found that all tests, except for the difference between the inside and outside of the J-ring and the rocking device, had good measurement capabilities and could detect differences between the two mixtures.

In general, the tests' repeatability decreased with increasing the concrete flow. Nevertheless, tests with acceptable reproducibility will still have more than 5% accuracy.

This research observed dynamic stability during the concrete flow due to its weight and without external energy. In contrast, dynamic stability versus external energy (such as the impact introduced into the mold) depends more on static stability and cement content factors. In order to study the second case, the rocking system is suggested, where the P1 index can be used instead of conducting surface infiltration experiments.

Due to the proper relationship between surface infiltration experiments, a modified probe with no symmetry of the probe system and the more expensive fabrication of the penetration test apparatus can be used instead of these two experiments. Additionally, the relationship between surface infiltration experiments and column tests is recommended using a modified probe with a critical value of 6 mm instead of the separation column test.

In addition, to simplify and use the separation column experiment, sieve number 3.8 can be used instead of sieve number 4 when sifting the aggregates and increasing the limit of the calculated critical index needed to confirm the stability of concrete from 10 to 15.

In the modified L-box test, it is possible to test the experiment by applying changes in the calculation of the relevant index to the initial offer and the possibility of using sieve number 3.8 instead of sieve number 4.

In casting a beam mold, it was observed that instability has the most effect on the specific electrical concrete resistance, so the average of this variable in the beam made with unstable concrete is 32% more than the average value in the beam made with stable concrete. In addition, the uniform specific electrical resistance distribution in the unstable beam is much higher than in the beam made with stable concrete, so this variable was reduced by 58% in the beam with unstable concrete. In contrast, there is a 21% decrease in the beam with stable concrete.

In investigating the effect of instability on the apparent density distribution in the volume of the beams made with two different types of concrete, it was seen that instability could reduce the density to some extent of $Kg/m^3$ at the points far from the casting point.

Instability in concrete can reduce the compressive strength of a concrete slab with the cement content and the water-to-cement ratio by 9%. Moreover, in the beam made with stable concrete, the compressive strength was decreased by increasing the distance from the casting point. In addition to 1.5 m concrete, compressive strength loss will be 30%. For this reason, it is recommended to restrict the distances between the casting points in the implementation.

## CRediT authorship contribution statement

**Fazel Azarhomayun:** Data curation, Investigation, Conceptualization, Methodology, Validation, Formal analysis, Writing - original draft, Writing - review & editing. **Mohammad Haji:** Investigation, Visualization, Writing – review & editing, Writing – original draft. **Mohammad Shekarchi:** Conceptualization, Supervision, Methodology, Writing – review & editing. **Mahdi Kioumarsi:** Conceptualization, Supervision, Resources, Visualization, Project administration, Investigation, Methodology, Validation, Writing - original draft, Writing - review & editing.

## Declaration of Competing Interest

The authors declare that they have no known competing financial interests or personal relationships that could have appeared to influence the work reported in this paper.

## Data availability

Data will be made available on request.

## References

[1] ACI 237R-07, "Self-consolidating concrete", ACI Manual of Concrete Practice, Part 1, American Concrete Institute, Farmington Hills, Michigan, USA, 2007, p. 30 pp.
[2] K.H. Khayat, Y. Vanhove, T.V. Pavate, C. Jolicoeur, Multi-electrode conductivity method to evaluate static stability of flowable and self-consolidating concrete, ACI Mater. J. 104 (2007) 424.
[3] K.H. Khayat, Workability, testing, and performance of self-consolidating concrete, Mater. J. 96 (1999) 346–353.
[4] R.S. Ravindrarajah, D. Siladyi, B. Adamopoulos. Development of high-strength self-compacting concrete with reduced segregation potential. Proc. 3rd Int. RILEM Symp. Reykjavik, Icel., vol. 1, 2003, p. 1048.
[5] D. Bonen, S.P. Shah, Fresh and hardened properties of self-consolidating concrete, Prog. Struct. Eng. Mater. 7 (2005) 14–26.
[6] J. Assaad, K.H. Khayat, J. Daczko, Evaluation of static stability of self-consolidating concrete, Mater. J. 101 (2004) 207–215.
[7] H.A. Mesbah, A. Yahia, K.H. Khayat, Electrical conductivity method to assess static stability of self-consolidating concrete, Cem. Concr. Res. 41 (2011) 451–458, https://doi.org/10.1016/j.cemconres.2011.01.004.
[8] ASTM C1610/C1610M-19, Standard Test Method for Static Segregation of Self-Consolidating Concrete Using Column Technique, ASTM International, West Conshohocken, PA, 2019.
[9] V.K. Bui, D. Montgomery, I. Hinczak, K. Turner, Rapid testing method for segregation resistance of self-compacting concrete, Cem. Concr. Res. 32 (2002) 1489–1496, https://doi.org/10.1016/S0008-8846(02)00811-6.
[10] L. Shen, L. Struble, D. Lange. Testing static segregation of SCC. SCC2005, Proc. 2nd North Am. Conf. Des. Use SCC, Novemb., 2005, p. 1–3.
[11] T.V. Pavate, K.H. Khayat, C. Jolicoeur, In-situ conductivity method for monitoring segregation, bleeding, and strength development in cement-based materials, Spec. Publ. 195 (2000) 535–560.
[12] H. El-Chabib, M. Nehdi, Effect of mixture design parameters on segregation of self-consolidating concrete, ACI Mater. J. 103 (2006) 374.
[13] L. Shen, H.B. Jovein, M. Li, Measuring static stability and robustness of self-consolidating concrete using modified Segregation Probe, Constr. Build. Mater. 70 (2014) 210–216, https://doi.org/10.1016/j.conbuildmat.2014.07.112.
[14] L. Shen, L. Struble, D. Lange, Modeling static segregation of self-consolidating concrete, ACI Mater. J. 106 (2009) 367.
[15] A.W. Saak, H.M. Jennings, S.P. Shah, New methodology for designing self-compacting concrete, Mater. J. 98 (2001) 429–439.
[16] Astm C1611/C1611M-18, Standard Test Method for Slump Flow of Self-Consolidating Concrete, ASTM International, West Conshohocken, PA, 2018.
[17] ASTM C1621/C1621M-17, Standard Test Method for Passing Ability of Self-Consolidating Concrete by J-Ring, ASTM International, West Conshohocken, PA, www.astm.org. 2017. doi:10.1520/C1621_C1621M-17.
[18] EFNARC, "Specification and Guidelines for Self-Compacting Concrete,2002.".
[19] Structures TCS-CCIU of T and RL for M and. Self-compacting concrete: state-of-the-art report of RILEM Technical Committee 174-SCC, Self-Compacting Concrete. RILEM Publ.; 2000.
[20] P.J.M. Bartos, M. Sonebi, A.K. Tamimi, Report 24: workability and rheology of fresh concrete: compendium of tests–report of RILEM Technical Committee TC 145-WSM, vol. 24, RILEM publications, 2002.
[21] P. Turgut, K. Türk, H. Bakırcı. A New Test Method for Dynamic Segregation Resistance of Self-Consolidating Concrete using L-box Apparatus. 10th Int. Congr. Adv. Civ. Eng. Ankara, Turkey 2012.

[22] G. Wang, Y. Kong, T. Sun, Z. Shui, Effect of water–binder ratio and fly ash on the homogeneity of concrete, Constr. Build. Mater. 38 (2013) 1129–1134, https://doi.org/10.1016/j.conbuildmat.2012.09.027.
[23] H.S. Gökçe, Ö. Andiç-Çakır, A dynamic segregation test method for heavyweight concrete: density variation method, J. Test. Eval. 48 (2020) 20180196, https://doi.org/10.1520/JTE20180196.
[24] N. Tregger, A. Gregori, L. Ferrara, S. Shah, Correlating dynamic segregation of self-consolidating concrete to the slump-flow test, Constr. Build. Mater. 28 (2012) 499–505, https://doi.org/10.1016/j.conbuildmat.2011.08.052.
[25] L. Shen, L. Struble, D. Lange. Measuring dynamic segregation of SCC. Proc., Third North Am. Conf. Des. Use Self-Consolidating Concr. (SCC), Curran Assoc. New York., 2008.
[26] B. Esmaeilkhanian, K.H. Khayat, A. Yahia, D. Feys, Effects of mix design parameters and rheological properties on dynamic stability of self-consolidating concrete, Cem. Concr. Compos. 54 (2014) 21–28, https://doi.org/10.1016/j.cemconcomp.2014.03.001.
[27] F. Azarhomayun, M. Haji, M. Kioumarsi, M. Shekarchi, Effect of calcium stearate and aluminum powder on free and restrained drying shrinkage, crack characteristic and mechanical properties of concrete, Cem. Concr. Compos. 125 (2022), 104276, https://doi.org/10.1016/j.cemconcomp.2021.104276.
[28] K. Khayat, J. Assaad, J. Daczko, Comparison of field-oriented test methods to assess dynamic stability of self-consolidating concrete, ACI Mater. J. 101 (2) (2004).
[29] B. Felekoğlu, S. Türkel, B. Baradan, Effect of water/cement ratio on the fresh and hardened properties of self-compacting concrete, Build. Environ. 42 (4) (2007) 1795–1802.
[30] L. Ferrara, Y. Park, S. Shah, A method for mix-design of fiber-reinforced self-compacting concrete, Cem. Concr. Res. 37 (6) (2007) 957–971.
[31] M. Mouret, G. Escadeillas, A. Bascoul, Metrological significance of the column test in the assessment of the static segregation of self-compacting concrete in the fresh state, Mater. Struct. 41 (4) (2007) 663–679.
[32] W. Elemam, A. Abdelraheem, M. Mahdy, A. Tahwia, Optimizing fresh properties and compressive strength of self-consolidating concrete, Constr. Build. Mater. 249 (2020), 118781, https://doi.org/10.1016/j.conbuildmat.2020.118781.
[33] A. Patel, P. Bhuva, E. George, D. Bhatt. Compressive strength and modulus of elasticity of self-compacting concrete. National conference on Recent trends in Engineering and Technology. 2011.
[34] C. Shi, Z. Wu, K. Lv, L. Wu, A review on mixture design methods for self-compacting concrete, Constr. Build. Mater. 84 (2015) 387–398.
[35] M. Mahoutian, M. Shekarchi, Effect of inert and pozzolanic materials on flow and mechanical properties of self-compacting concrete, J. Mater. (2015) 1–11.
[36] F. Benmerioul, A. Makani, A. Tafraoui, S. Zaouai, Valorization of the crushed dune sand in the formulation of self-compacting-concrete, Procedia Eng. 171 (2017) 672–678.
[37] I. Mehdipour, M.S. Razzaghi, K. Amini, M. Shekarchi, Effect of mineral admixtures on fluidity and stability of self-consolidating mortar subjected to prolonged mixing time, Constr. Build. Mater. 40 (2013) 1029–1037, https://doi.org/10.1016/j.conbuildmat.2012.11.108.
[38] N. Thakre, D. Mangrulkar, M. Janbandhu, J. Saxena, Self-compacting concrete - Robustness of SCC, Int. J. Adv. Eng. Res. Sci. 4 (3) (2017) 138–141.
[39] I. González-Taboada, B. González-Fonteboa, J. Eiras-López, G. Rojo-López, Tools for the study of self-compacting recycled concrete fresh behaviour: workability and rheology, J. Clean. Prod. 156 (2017) 1–18.
[40] A. Anil Thakare, S. Siddique, S. Sarode, R. Deewan, V. Gupta, S. Gupta, S. Chaudhary, A study on rheological properties of rubber fiber dosed self-compacting mortar, Constr. Build. Mater. 262 (2020), 120745.
[41] W. Yan, W. Cui, L. Qi, Effect of aggregate gradation and mortar rheology on static segregation of self-compacting concrete, Constr. Build. Mater. 259 (2020), 119816.
[42] A. Suprakash, S. Karthiyaini, M. Shanmugasundaram, Future and scope for development of calcium and silica rich supplementary blends on properties of self-compacting concrete - A comparative review, J. Mater. Res. Technol. 15 (2021) 5662–5681.
[43] S. Pan, D. Chen, X. Chen, G. Ge, D. Su, C. Liu, Experimental study on the workability and stability of steel slag self-compacting concrete, Appl. Sci. 10 (4) (2020) 1291.
[44] H. Li, F. Huang, Z. Yi, Z. Wang, Y. Zhang, Z. Yang, Investigations of mixing technique on the rheological properties of self-compacting concrete, Appl. Sci. 10 (15) (2020) 5189.
[45] B. Mohamed. Effect of coarse aggregates and sand contents on workability and static stability of self-compacting concrete. Koreascience.or.kr, 2022.
[46] F. Aghziel Sadfa, M. Ben Aicha, M. Zaher, A. Hafidi Alaoui, Y. Burtschell, New test for the determination of static segregation of self-compacting concrete: three-circles test, Mater. Today: Proc. 62 (2022) 4161–4167.
[47] M. Geiker, S. Jacobsen, Self-compacting concrete (SCC), in: Developments in the Formulation and Reinforcement of Concrete, Woodhead Publishing, 2019, pp. 229–256.
[48] Y. Liu, S. Hou, C. Li, H. Zhou, F. Jin, P. Qin, Q. Yang, Study on support time in double-shield TBM tunnel based on self-compacting concrete backfilling material, Tunnel. Underground Space Technol. 96 (2020), 103212.
[49] ASTM C150/C150M-19a, Standard Specification for Portland Cement; ASTM International: West Conshohocken, PA, USA, 2019.
[50] ASTM. Standard Test Method for Sieve Analysis of Fine and Coarse Aggregates, ASTM C136, Annual Book of American Society for Testing Materials Standards, Vol. C 04.02. (2006).
[51] American Society for Testing and Materials. Standard Specification for Concrete Aggregates ASTM C33/C33 M-16; American Society for Testing and Materials: West Conshohocken, PA, USA, 2016.
[52] ASTM C192, Standard Practice for Making and Curing Concrete Test Specimens in the Laboratory, ASTM Int. West Conshohocken, 2006.
[53] ASTM C1611/C1611M-05, "Standard Test Method for Slump Flow of Self-Consolidating Concrete," ASTM International, West Conshohocken, PA., 2005.
[54] ASTM C 1610/C 1610M-06 "Standard Test Method for Static Segregation of Self-Consolidating Concrete Using Column Technique," ASTM International.
[55] ASTM C1621/C1621M-06, Standard Test Method for Passing Ability of Self-Consolidating Concrete by J-Ring, ASTM International: West Conshohocken, PA., 2006.
[56] P. Turgut, K Türk, H.Bakırcı, "A New Test Method for Dynamic Segregation Resistance of Self-Consolidating Concrete using L-box Apparatus", 10th International Congress on Advances in Civil Engineering, Middle East Technical University, Ankara, Turkey, October 2012.
[57] L. Shen, H. Bahrami Jovein, M. Li. Measuring static stability and robustness of self-consolidating concrete using modified Segregation Probe, Constr. Build. Mater. 70 2014 210–216.
[58] L. Shen, H. Bahrami Jovein, M. Li. Measuring static stability and robustness of self-consolidating concrete using modified Segregation Probe, Constr. Build. Mater. 70 2014 210–216.
[59] ASTM C1712-09, Standard test method for rapid assessment of static segregation resistance of self-consolidating concrete using penetration test, American Society for Testing and Materials, 2009.
[60] B. Esmaeilkhanian, D. Feys, K.H. Khayat, A. Yahia, New test method to evaluate dynamic stability of self consolidating concrete, ACI Mater. J. (2014) 299–308.
[61] Standard Guide for Conducting a Repeatability and Reproducibility Study on Test Equipment for Nondestructive Testing (Withdrawn 2018).
[62] ASTM C 642 – 97, "Standard Test Methods for Density, Absorption and Voids in Hardened Concrete" ASTM International.